

OF RODENTS AND RANDOMNESS: MACROECOLOGICAL APPROACHES TO
COMMUNITY STRUCTURE

By

RENATA M. DIAZ

A DISSERTATION PRESENTED TO THE GRADUATE SCHOOL
OF THE UNIVERSITY OF FLORIDA IN PARTIAL FULFILLMENT
OF THE REQUIREMENTS FOR THE DEGREE OF
DOCTOR OF PHILOSOPHY

UNIVERSITY OF FLORIDA

2022

© 2022 Renata M. Diaz

To R , K , r , and h .

ACKNOWLEDGEMENTS

I will always be grateful to my dissertation advisor, Morgan Ernest, and my committee, Ethan White, Jamie Gillooly, and Justin Kitzes, for five years' of support and guidance as I have found my way through these projects. Throughout this journey, my mentors have consistently given me the encouragement and freedom to pursue challenging and adventurous projects, and modeled an approach to science grounded in curiosity, kindness, and bravery. I hope to bring a similar spirit to my future endeavors.

I am equally grateful to the ones who have shared this path with me over the years. In particular: Hao Ye, for being a steady and wise teacher on topics ranging from computational ecology, to cycling, to combinatorics; Ellen Bledsoe, for being a role model and a friend, from my very first weeks as a weecologist; Sam Zlotnik, for long walks and an appreciation for creatures; Pat Dumandan, for bringing joy and fresh perspective to the lab; and especially Jerald Pinson, for sharing stillness, wonder, and mirth.

Fundamentally, this dissertation is for my family. My mother, Katie, is a scientist in the purest way, and perpetually inspires me to find something new to explore in the natural world. My father, Ricardo, taught me that no matter how abstract or sophisticated a theory may seem, on some level it is about rats; and that sometimes a bicycle holds more answers than a supercomputer. My sister, Rosalind, brings wisdom and lightness to every challenge, and I am grateful every day that there are two of us. Finally, Hatter never forgets to remind me to love the little things in life, and gives me a reason to come home even on the darkest nights.

TABLE OF CONTENTS

	<u>page</u>
ACKNOWLEDGEMENTS	4
LIST OF TABLES.....	8
LIST OF FIGURES.....	9
LIST OF OBJECTS	10
LIST OF ABBREVIATIONS.....	11
ABSTRACT	12
CHAPTER	
1 INTRODUCTION	14
2 MAINTENANCE OF COMMUNITY FUNCTION THROUGH COMPENSATION BREAKS DOWN OVER TIME IN A DESERT RODENT COMMUNITY	16
2.1 Background	16
2.2 Methods.....	18
2.2.1 The Portal Project	18
2.2.2 Data.....	19
2.2.3 Statistical analysis of rodent community energy use and biomass	19
2.3 Results	21
2.4 Discussion.....	22
3 TEMPORAL CHANGES IN THE INDIVIDUAL SIZE DISTRIBUTION DECOUPLE LONG-TERM TRENDS IN ABUNDANCE, BIOMASS, AND ENERGY USE OF NORTH AMERICAN BREEDING BIRD COMMUNITIES	27
3.1 Background	27
3.2 Methods.....	29
3.2.1 Bird abundance data.....	29
3.2.2 Estimated size data	30
3.2.3 Comparing abundance- and size- based currencies	31
3.2.4 Long-term trends.....	32
3.2.5 Relating change in community structure to decoupling between individual- and size-based dynamics.....	33
3.3 Results	35
3.4 Discussion.....	36
3.4.1 Abundance, biomass, and energy use are nonequivalent currencies	36
3.4.2 For North American breeding birds, biomass has declined less than abundance or energy use.....	37
3.4.3 Complex relationships between compositional change and community-level properties	38
3.4.4 Conclusion.....	39

4	EXAMPLES OF EDITOR/AUTHOR TOOLS, TABLES, AND IMAGES	41
4.1	Example of using the authorRemark and editorRemark	41
4.2	Table Examples	41
4.3	Very Long Tables	41
4.4	Examples of Adding Graphics	45
4.5	A Note on Graphics	47
4.6	Placement Specifiers	48
5	SUMMARY AND CONCLUSIONS	49
5.1	Non Porttitor Tellus	49
5.1.1	Nam Arcu Magna	49
5.1.2	Nam Arcu Magna	49
5.2	Non Porttitor Tellus	50
APPENDIX		
A	SUPPLEMENTAL RESULTS AND ANALYSES FOR CHAPTER 2	51
A.1	Plot-level analysis	51
A.1.1	Explanation	51
A.1.2	Compensation	51
A.1.3	Total energy use	51
A.1.4	<i>Dipodomys</i> proportional energy use	52
A.1.5	<i>C. baileyi</i> proportional energy use	52
A.1.6	Tables	53
A.2	Full model results	56
A.2.1	Compensation	56
A.2.2	Total energy use ratio	56
A.2.3	<i>Dipodomys</i> proportional energy use	57
A.2.4	<i>C. baileyi</i> proportional energy use	57
A.2.5	Tables	58
A.3	Biomass analysis	60
A.3.1	Compensation	60
A.3.2	Total biomass ratio	61
A.3.3	<i>Dipodomys</i> proportional biomass	61
A.3.4	<i>C. baileyi</i> proportional biomass	61
A.3.5	Tables	62
A.4	Covariates of rodent community change	65
B	SECONDARY APPENDIX CONTENT	67
REFERENCES		68
BIOGRAPHICAL SKETCH		74

LIST OF TABLES

<u>Tables</u>	<u>page</u>
4-1 An example of a table caption in the incorrect place.....	41
4-2 A proper table caption location	42
4-3 Feasible triples for highly variable Grid, MLMMH.	42
4-4 Duplicate of Previous table, using longtables environment.....	44
4-5 Specifier Table	48
A-1 Plot-level: Model comparison for compensation.	53
A-2 Plot-level: Coefficients from linear mixed-effects model for compensation.	53
A-3 Plot-level: Estimates from linear mixed-effects model for compensation.	53
A-4 Plot-level: Contrasts from linear mixed-effects model for compensation.....	53
A-5 Plot-level: Model comparison for total energy use.	54
A-6 Plot-level: Coefficients from linear mixed-effects model for total energy ratio.	54
A-7 Plot-level: Estimates from linear mixed-effects model for total energy ratio.	54
A-8 Plot-level: Contrasts from linear mixed-effects model for total energy ratio.....	54
A-9 Plot-level: Model comparison for kangaroo rat proportional energy use.	54
A-10 Plot-level: Coefficients from GLMER on kangaroo rat energy use.	55
A-11 Plot-level: Estimates from GLMER on kangaroo rat energy use.....	55
A-12 Plot-level: Contrasts from GLMER on kangaroo rat energy use.....	55
A-13 Plot-level: Model comparison for <i>C. baileyi</i> proportional energy use.....	55
A-14 Plot-level: Coefficients from GLMER on <i>C. baileyi</i> energy use.	55
A-15 Plot-level: Estimates from GLMER on <i>C. baileyi</i> energy use.	56
A-16 Plot-level: Contrasts from GLMER on <i>C. baileyi</i> energy use.....	56
A-17 Model comparison for compensation.....	58
A-18 Coefficients from GLS model for compensation.	58
A-19 Estimates from GLS for compensation.	58
A-20 Contrasts from GLS for compensation.....	58
A-21 Model comparison for total energy use.	58
A-22 Coefficients from GLS for total energy ratio.	58
A-23 Estimates from GLS for total energy ratio.	59

A-24 Contrasts from GLS for total energy ratio.	59
A-25 Model comparison for kangaroo rat proportional energy use.	59
A-26 Coefficients from GLM on kangaroo rat energy use.	59
A-27 Estimates from GLM on kangaroo rat energy use.	59
A-28 Contrasts from GLM on kangaroo rat energy use.	59
A-29 Model comparison for <i>C. baileyi</i> proportional energy use.	60
A-30 Coefficients from GLM on <i>C. baileyi</i> energy use.	60
A-31 Estimates from GLM on <i>C. baileyi</i> energy use.	60
A-32 Contrasts from GLM on <i>C. baileyi</i> energy use.	60
A-33 Model comparison for compensation.	62
A-34 Coefficients from GLS model for compensation.	62
A-35 Estimates from GLS for compensation.	62
A-36 Contrasts from GLS for compensation.	62
A-37 Model comparison for total biomass.	63
A-38 Coefficients from GLS for total biomass ratio.	63
A-39 Estimates from GLS for total biomass ratio.	63
A-40 Contrasts from GLS for total biomass ratio.	63
A-41 Model comparison for kangaroo rat proportional biomass.	63
A-42 Coefficients from GLM on kangaroo rat biomass.	63
A-43 Estimates from GLM on kangaroo rat biomass.	64
A-44 Contrasts from GLM on kangaroo rat biomass.	64
A-45 Model comparison for <i>C. baileyi</i> proportional biomass.	64
A-46 Coefficients from GLM on <i>C. baileyi</i> biomass.	64
A-47 Estimates from GLM on <i>C. baileyi</i> biomass.	64
A-48 Contrasts from GLM on <i>C. baileyi</i> biomass.	65
B-1 A sample Table using tabularx.	67

LIST OF FIGURES

<u>Figures</u>	<u>page</u>
2-1 Dynamics of energy use and rodent community composition over time.....	26
4-1 This is my shortened caption for my Table of Contents	46
4-2 This is my shortened caption for my Table of Contents	47
A-1 Changes in overall community energy use (A), NDVI (B), and local climate (C) surrounding the 2010 shift in rodent community composition.....	66
B-1 Figure Caption	67

LIST OF OBJECTS

Objects

page

LIST OF ABBREVIATIONS

AICc	Akaike information criterion adjusted for small sample sizes
<i>CB</i>	<i>Chaetodipus baileyi</i>
CB_C	Total metabolic flux of <i>Chaetodipus baileyi</i> on control plots
CB_E	Total metabolic flux of <i>Chaetodipus baileyi</i> on exclosure plots
E_{tot}	Total community-wide metabolic flux
E_{totC}	Total community-wide metabolic flux on control plots
E_{totE}	Total community-wide metabolic flux on exclosure plots
GLS	Generalized least squares
GLM	Generalized linear model
ISD	Individual size distribution
<i>KR</i>	Kangaroo rat (<i>Dipodomys spp.</i>)
KR_C	Total metabolic flux of kangaroo rats on control plots
KR_E	Total metabolic flux of kangaroo rats on exclosure plots
SAD	Species abundance distribution
<i>SG</i>	Small granivore
SG_C	Total metabolic flux of small granivores on control plots
SG_E	Total metabolic flux of small granivores on exclosure plots

Abstract of Dissertation Presented to the Graduate School
of the University of Florida in Partial Fulfillment of the
Requirements for the Degree of Doctor of Philosophy

OF RODENTS AND RANDOMNESS: MACROECOLOGICAL APPROACHES TO
COMMUNITY STRUCTURE

By

Renata M. Diaz

August 2022

Chair: S. K. Morgan Ernest

Major: Interdisciplinary Ecology

The system-wide attributes of ecological communities - such as community-level abundance, biomass, and metabolic flux, and how these are distributed among species and organisms - emerge from a web of shifting environmental constraints, diverse species interactions, and ubiquitous mathematical rules. While this apparent complexity can present a challenge to synthesis in community ecology, a macroecological perspective embraces ecological complexity as a path towards general understanding. In this dissertation, I use a telescoping macroecological perspective to explore how these factors shape community properties and determine how they change over time, building from a granular focus on species interactions in a well-studied experimental system, to successively broader spatial and conceptual scales in pursuit of general insights. In chapter 1 (the introduction), I offer an overview of the macroecological approach as it applies to community ecology and the specific vignettes in this dissertation. In chapter 2, I use a long-term experiment on desert rodents to disentangle how shifting environmental conditions and species interactions modulate the impact of species loss on community function. In chapter 3, I leverage modern computational approaches to show how changes in community structure modulate nuanced relationships between the long-term trends in size- and individuals- based currencies of community function. In chapter 4, I borrow tools and conceptual frameworks from statistical mechanics to explore what common ecological patterns stand to teach us about ecological, as opposed to statistical, processes. Finally, in chapter 5 (the conclusion), I offer

concluding reflections on the current landscape of prospects and challenges associated with a macroecological lens on community structure and function.

CHAPTER 1 INTRODUCTION

The interplay between system-specific natural history narratives and ubiquitous ecological or even mathematical rules that combine to determine how abundance, biomass, and resource use are distributed among species and organisms and across different levels of organization in ecological communities lies at the core of community ecology [41, 5]. A macroecological approach integrates classic modalities of ecological inquiry with conceptual frameworks drawn from across the scope of complex systems studies to disentangle phenomena specific to particular systems from general phenomena that reflect processes that operate across diverse taxonomic, geographic, and temporal contexts [4, 46]. In this dissertation, I adopt a macroecological perspective to understanding the structure and function of ecological communities, working from a narrow, system-specific focus on a well-studied long-term experiment, to a broad taxonomic and conceptual perspective on the interplay between combinatorics, statistical mechanics, and community ecology.

In chapter 2 [12], I use 30 years' of accumulated data and natural history knowledge to explore the effects of species loss on community function in an experimentally manipulated desert rodent community. Understanding how community function responds to species loss, and how the effects of species loss interact with shifting environmental conditions, is a key problem for biodiversity science in the current era of unprecedented ecological change. In this system, compensation due to functional redundancy temporarily buffered community function against species loss [19]. However, because similar, but non-identical, rodent species have responded differently to changes in environmental conditions over time, this compensatory effect has broken down, leaving community function highly sensitive to the loss of keystone species.

In chapter 3, I undertake a continental-scale comparison across communities to explore how shifts in community-wide body size modulate the long-term dynamics of individual abundance, biomass, and energy use in North American breeding birds. Although individual abundance and size and energy-based currencies are intrinsically linked, they capture different dimensions of community function, and shifts in community size structure can decouple the dynamics of different currencies [72, 31, 53]. I find that, in nearly one third of communities, changes in the

community size structure result in qualitatively different trajectories for biomass and total abundance over the past 30 years. As a result, while trends in individual abundance are dominated by declines, trends in total biomass are evenly split between declines and increases.

In chapter 4 [13], I step further back to examine how fundamental mathematical constraints inform our understanding of ecological "laws". Common patterns in community ecology, such as the "hollow-curve" or J-shaped species abundance distribution (SAD), emerge from a combination of biological processes and ubiquitous mathematical constraints on the emergent properties of complex systems [51, 44]. Disentangling the signal of ecological processes from these mathematical constraints can provide new sources of inferential power linking pattern to process in community ecology [29]. I use combinatorics to characterize the mathematical constraint on the SAD, and compare the SADs of 22,000 empirically-observed communities to these "statistical baselines". This reveals that, while empirical SADs often match their statistical baselines, a substantial minority of real SADs deviate from these baselines - leaving an important role for ecological processes in shaping these distributions.

CHAPTER 2

MAINTENANCE OF COMMUNITY FUNCTION THROUGH COMPENSATION BREAKS DOWN OVER TIME IN A DESERT RODENT COMMUNITY

2.1 Background

Determining the extent to which community-level properties are affected by species loss, and how and why this changes over time, is key for understanding how communities are structured and how community function may respond to future perturbations [27]. When species are lost from a community, their contributions to community function (e.g. total productivity or resource use) are also directly lost. Community function may be maintained, however, if in the new community context, species that remain perform similar functions to the species that were lost, and compensate for the decline in function directly caused by species loss - i.e., functional redundancy [69, 68, 19, 57, 27]. When compensation via functional redundancy occurs among consumers with a common resource base, it is consistent with a zero-sum competitive dynamic, in which resources not used by one species are readily absorbed by competitors, and any increases in the abundance of one species must come at the direct expense of others [67, 20].

Because the response of system-level function to species loss is partially determined by the degree of functional redundancy in a community, processes that cause functional redundancy to change over time can have important consequences for the long-term maintenance of ecosystem function. Colonization events may buffer community function against species loss, if a community gains species that perform similar functions to the species that were lost [19, 42]. The ability of colonization to supply functionally redundant species depends on the species (and traits) present in the broader metacommunity, and on the rate of dispersal supplying appropriate species to local communities [42].

Even without the addition of new species and traits, however, functional redundancy within a consistent set of coexisting species may fluctuate over time. While, in theory, functional redundancy may occur via the special case of complete niche neutrality (e.g. [34]), it may also occur in niche-structured systems that contain species that share some traits but differ along other niche axes [65]. In these systems, if similar, but non-identical, species respond to environmental change in similar ways, functional overlap can be maintained or even strengthened. However, if

niche differences cause species to respond differently to changing conditions, the degree of functional overlap between those species may decline, resulting in a breakdown in compensation [45, 23]. Over time, as metacommunity dynamics and changing environmental conditions modulate functional redundancy within a community, the extent to which community function is robust to species loss - and the strength of zero-sum competition - may also be dynamic and context-dependent.

Despite logical conceptual support, and evidence from experimental microcosms [23], there is little empirical documentation of how, and through which mechanisms, temporal changes in functional redundancy modulate the effect of species loss on ecosystem function in natural assemblages. Although relatively plentiful, observational data cannot unambiguously detect compensation through functional redundancy, and even short-term experiments may not be sufficient to capture temporal variation in compensation [19, 33]. In contrast, long-term manipulative experiments are uniquely suited to address this question. In long-term experiments in which key species are removed from a community over an extended period of time, the impact of species loss on community function can be directly quantified by comparing community function between complete and manipulated assemblages. As metacommunity dynamics and environmental conditions shift over time, long-term monitoring can reveal how these processes contribute to changes in functional redundancy and ecosystem function across different time periods. Due to the financial and logistical resources required to maintain and monitor whole-community manipulations over long timescales, these experiments are rare in natural systems representative of realistic evolutionary, geographic, and environmental constraints [35].

Here, we use a 30-year experiment on desert rodents to investigate how shifts in functional redundancy alter the effect of species loss on community function over time. In this study, kangaroo rats (*Dipodomys* spp.), the largest and competitively dominant species in the rodent community, have been removed from a subset of experimental plots to explore how the loss of key species affects community function, measured as community-level metabolic flux (“total energy use”, or E_{tot}) or total biomass [22]. For systems of consumers with a shared resource

base, such as this community of granivorous rodents, E_{tot} reflects the total amount of resources being processed by an assemblage, and total biomass directly reflects standing biomass. Both are important metrics of community function [40, 19]. Long-term monitoring of this experiment has documented repeated shifts in the habitat and species composition of this system, resulting in distinct time periods characterized by different habitat conditions and configurations of the rodent community [8]. Abrupt reorganization events in community composition occurred in 1997 and in 2010, associated with the establishment and subsequent decline of the pocket mouse *Chaetodipus baileyi*. *C. baileyi* is similar in size, and presumably other traits, to kangaroo rats, and its establishment in 1996-97 drove a pronounced increase in compensation due to functional redundancy between *C. baileyi* and kangaroo rats [19, 65]. Over the course of this experiment, shifting environmental conditions have caused the habitat at the study site to transition from desert grassland to scrub, driving a shift in baseline rodent community composition away from kangaroo rats and favoring other, smaller, granivores [3, 20]. By making comparisons across these time periods, we explored how shifts in community composition and functional overlap among the same species have contributed to long-term changes in the effect of species loss on community function.

2.2 Methods

2.2.1 The Portal Project

The Portal Project consists of a set of 24 fenced experimental plots located approximately 7 miles east of Portal, AZ, USA, on unceded land of the Chiricahua Apache. Beginning in 1977, kangaroo rats (*Dipodomys spectabilis*, *D. merriami*, and *D. ordii*) have been experimentally excluded from a subset of these plots (exclosures), while all other rodents are allowed access through small holes cut in the plot fencing. Control plots, with larger holes, are accessible to all rodents, including kangaroo rats. Rodents on all plots are censused via monthly bouts of live-trapping. Each individual captured is identified to species and weighed. For additional details on the site and methodology of the Portal Project, see [22].

2.2.2 Data

We used data for control and exclosure plots from February 1988 until January 2020. The experimental treatments for some plots have changed over time, and we used the subset of plots that have had the same treatments for the longest period of time [22]. Four control plots, and five exclosure plots, met these criteria. In order to achieve a balanced sample, we randomly selected four exclosure plots for analysis. We divided the timeseries into three time periods defined by major transitions in the rodent community surrounding the establishment and decline of *C. baileyi* [19, 8]. The first time period (February 1988-June 1997) precedes *C. baileyi*'s establishment at site. We defined *C. baileyi*'s establishment date as the first census period in which *C. baileyi* was captured on all exclosure plots (following [2]). During the second time period (July 1997-January 2010), *C. baileyi* was abundant on both exclosure and control plots. This time period ended with a reorganization event in which *C. baileyi* became scarce sitewide. We used January 2010, the midpoint of the 95% credible interval for the date of this reorganization event as estimated in [8], as the end date for this time period. The last time period spans from February 2010-January 2020. For each individual rodent captured, we estimated the individual-level metabolic rate using the scaling relationship between individual body mass and metabolic rate $b = 5.69 * (m^{0.75})$, where m is body mass in grams and b is metabolic rate (for details, see [72]). We calculated treatment and species-level energy use as the sum of the appropriate individuals' metabolic rates, and total biomass as the sum of individuals' body mass measurements.

2.2.3 Statistical analysis of rodent community energy use and biomass

Here, we describe analyses for energy use. For biomass, we repeated these analyses substituting biomass values for energy use throughout. For all variables, we combined data for all plots within a treatment in each monthly census period and calculated treatment-level means. This is necessary to calculate compensation, and we treated other variables in the same way to maintain consistency. A provisional plot-level analysis yielded qualitatively equivalent results (Appendix A). To measure the overall impact of kangaroo rat removal on E_{tot} , we calculated a “total energy ratio” as the ratio of treatment-level E_{tot} for kangaroo-rat exclosure plots relative to

unmanipulated control plots, i.e. E_{totE}/E_{totC} where E_{totE} and E_{totC} are total energy use on exclosures and controls, respectively [65, 2]. This ratio is distinct from compensation, which we defined as the proportion of the energy made available by kangaroo rat removal taken up via compensatory increases in energy use by small granivores (all granivores other than kangaroo rats; *Baiomys taylori*, *C. baileyi*, *Chaetodipus hispidus*, *Chaetodipus intermedius*, *Chaetodipus penicillatus*, *Perognathus flavus*, *Peromyscus eremicus*, *Peromyscus leucopus*, *Peromyscus maniculatus*, *Reithrodontomys fulvescens*, *Reithrodontomys megalotis*, and *Reithrodontomys montanus*). We calculated this as $(SG_E - SG_C)/KR_C$, where SG_E and SG_C are the amount of energy used by small granivores (SG) on exclosure and control plots, respectively, and KR_C is the amount of energy used by kangaroo rats (KR) on control plots [19]. To compare these variables across time periods, we used generalized least squares models (GLS; the R package *nlme* [54]) of the form $(SG_E - SG_C)/KR_C = timeperiod$, for compensation, and $E_{totE}/E_{totC} = timeperiod$, for the total energy ratio. We included a continuous-time autoregressive temporal autocorrelation term to account for temporal autocorrelation between values from monthly census periods within each multi-year time period (for details of model selection, see Appendix A). To evaluate change in baseline community composition over time, we calculated the proportion of treatment-level energy use accounted for by kangaroo rats on control plots in each census period (KR_C/E_{totC}). Proportional energy use is bounded 0-1 and is therefore not appropriate for GLS, so we compared values across time periods using a binomial generalized linear model (GLM) of the form $KR_C/E_{totC} = timeperiod$. Finally, we calculated the proportional energy use accounted for by *C. baileyi* (CB) on exclosure and control plots in each census period (CB_E/E_{totE} and CB_C/E_{totC} , respectively). *C. baileyi* was not present at the site prior to 1996, and we restricted the analysis of *C. baileyi* proportional energy use to the second two time periods. We compared *C. baileyi* proportional energy use over time and across treatments using a binomial GLM of the form $CB_E/E_{totE} = timeperiod + treatment$. For all models, we calculated estimated means and 95 confidence or credible intervals for time-period (and, for *C. baileyi*, treatment) level values, and contrasts between time periods (and, for *C. baileyi*, treatments), using the R package *emmeans*

[43]. Analyses were conducted in R 4.0.3 [55]. Data and code are archived at <https://doi.org/10.5281/zenodo.5544361> and <https://doi.org/10.5281/zenodo.5539880>.

2.3 Results

The impact of kangaroo rat removal on community function has changed repeatedly over time, through a combination of abrupt shifts in compensation associated with *C. baileyi*, and long-term changes in baseline community composition sitewide (Figure 2-1). These dynamics are qualitatively identical whether function is measured as total energy use (Figure 2-1; Appendix A) or total biomass (Appendix A). The first shift coincided with *C. baileyi*'s establishment in the community beginning in 1996-97 (Figure 2-1D). *C. baileyi* rapidly became dominant on exclosure plots and dramatically increased compensation (Figure 2-1B). From 1997-2010, small granivores compensated for an average of 58% of kangaroo rat energy use on control plots (95% interval 48-67%), an increase from an average of 18% from 1988-1997 (95% interval 8-29%; contrast $p < 0.001$; for complete results of all models, see Appendix A) from 1997-2010. With *C. baileyi*'s addition to the community, the total energy ratio (on exclosures relative to controls; Figure 2-1A) increased from 30% (20-40%) to 71% (62-79%, contrast $p = 0.014$). In the second shift, beginning around 2010, *C. baileyi*'s abundance sitewide dropped precipitously (Figure 2-1D). *C. baileyi*'s proportional energy use dropped from an average of 72% (65-80%) to 26% (18-35%, contrast $p < 0.001$) on exclosure plots, and from 11% (6-16%) to essentially 0 on control plots (contrast $p < 0.001$). Other species of small granivore did not make compensatory gains to offset the decline in *C. baileyi* (Figure 2-1B). As a result, compensation declined from an average of 58% (48-67%) to 28% (17-38%, contrast $p = 0.002$), a level not significantly different from the 18% (8-29%, contrast $p = .44$) observed prior to *C. baileyi*'s establishment at the site. Somewhat paradoxically, while the total energy ratio also dropped following *C. baileyi*'s decline, from an average of 71% (62-79%) from 1997-2010 to 50% (40-60%, contrast $p = 0.0056$) from 2010-2020, it remained higher than its average of 30% (20-40%, contrast $p = 0.0144$) from 1988-1997 (Figure 2-1A). Over the course of the experiment, community composition shifted sitewide. In later years, kangaroo rats accounted for a lower proportion of baseline E_{tot} than they

did at the beginning of the study (Figure 2-1C). From 1988-1997, kangaroo rats accounted for 92% (87-97%) of E_{tot} on controls; after 1997, this dropped to an average of approximately 70% (1988-1997 compared to later time periods, both $p = .0004$; 1997-2010 and 2020-2020 not significantly different, $p = .976$). Because the proportion of E_{tot} directly lost to kangaroo rat removal was smaller from 2010-2020 than from 1988-1997, the total energy ratio was higher from 2010-2020 than it was from 1988-1997 - even though there was not a detectable difference between the two time periods in the proportion of lost energy being offset through compensation.

2.4 Discussion

The dynamics of rodent community energy use at Portal illustrate that the role of functional redundancy in buffering community function against species loss fluctuates over time, due to changes in both species composition and in the degree of functional overlap among the same species. The 1997 increase in compensation, driven by *C. baileyi*'s establishment at the site, was a clear and compelling instance of colonization from the regional species pool overcoming limitations on functional redundancy [19, 42]. Although the small granivore species originally present in the community did not possess the traits necessary to compensate for kangaroo rats, *C. baileyi* supplied those traits and substantially, but incompletely, restored community function. In contrast, following the community reorganization event in 2010, *C. baileyi* remained present in the community, but ceased to operate as a partial functional replacement for kangaroo rats. This is consistent with fluctuating conditions modulating functional redundancy between similar, but non-identical, competitors. Kangaroo rats and *C. baileyi* are relatively similar in size and are demonstrably capable of using similar resources. However, *C. baileyi* prefers different, shrubbier microhabitats than kangaroo rats, and the two groups have been observed to replace each other in adjacent habitats [19]. We suggest that this study site, which has historically been dominated by kangaroo rats, constitutes marginal habitat for *C. baileyi*, and that, while conditions from 1997-2010 aligned sufficiently with *C. baileyi*'s requirements to create appreciable functional redundancy between kangaroo rats and *C. baileyi*, conditions since have caused this redundancy to break down. *C. baileyi*'s decline occurred immediately following a period of low plant

productivity and low rodent abundance community-wide, and in the decade following, the site experienced two long and severe droughts (Appendix A; [8]). These extreme conditions may themselves have limited *C. baileyi*'s fitness at the site, or the community-wide low abundance event may have temporarily overcome incumbency effects and triggered a community shift tracking longer-term habitat trends [64, 8]. Regardless of the proximate cause of *C. baileyi*'s decline, the fact that *C. baileyi* remains in the community, but no longer compensates for kangaroo rats, illustrates that changing conditions can have profound effects on community function by modulating the degree of functional redundancy within a consistent set of species.

While changes in compensation have contributed to changes in community function in this system, changes in compensation alone do not fully account for the long-term changes in the overall impact of kangaroo rat removal on *Etot*. Since 2010, although the ratio of *Etot* on exclosure plots relative to control plots declined coinciding with the breakdown in compensation associated with *C. baileyi*, it remained higher than the levels observed prior to 1997 (Figure 2-1A). This difference between the first and last time periods cannot be explained by an increase in compensation, as compensation from 2010-2020 was not greater than pre-1997 levels (Figure 2-1B). Rather, the increase in *Etot* on exclosure plots relative to control plots was the result of a long-term decrease in the contribution of kangaroo rats to *Etot* sitewide. Because kangaroo rats accounted for a smaller proportion of *Etot* on control plots from 2010-2020 than they did prior to 1997, their removal had a smaller impact on community function – even though there was not an increase in the degree to which small granivores compensated for their absence. In fact, the comparable levels of compensation achieved in the decades preceding and following *C. baileyi*'s dominance at the site suggest a relatively stable, and limited, degree of functional overlap between kangaroo rats and the original small granivores (i.e., excluding *C. baileyi*). Niche complementarity, combined with changing habitat conditions, may partially explain this phenomenon. It is well-documented that, while kangaroo rats readily forage in open microhabitats where predation risk can be relatively high, smaller granivores preferentially forage in sheltered microhabitats as an antipredator tactic [37]. Over the course of this experiment, the

habitat at this study site has transitioned from an arid grassland to a shrubland [3]. As sheltered microhabitats became more widespread, small granivores may have gained access to a larger proportion of resources and increased their share of *Etot* sitewide. However, kangaroo rats may have continued to use resources in open areas, which would have remained inaccessible to smaller granivores even on exclosure plots. The long-term reduction in the impact of kangaroo rat removal on community function, driven by niche complementarity and consistent niche partitioning, contrasts with the temporary compensatory dynamic driven by functional redundancy with *C. baileyi*. Although changes in the overall effect of species loss are sometimes treated interchangeably with compensation (e.g. [19] compared to [65]), it is important to recognize that multiple distinct pathways modulate the long-term impacts of species loss on community function. Particularly in strongly niche-structured systems, complementarity effects and fluctuations in functional redundancy may occur simultaneously, with complex and counterintuitive impacts on community function.

Overall, the decadal-scale changes in energy use among the Portal rodents underscore the importance of long-term metacommunity dynamics to the maintenance of community function following species loss (see [42]). Although a single colonization event may allow for temporary compensation via functional redundancy, as conditions shift, species that once compensated may no longer perform that function (see also [36]). Particularly if limiting similarity prevents similar competitors from specializing on precisely the same habitats [57], temporary, context-dependent compensation may be common. To maintain compensation over time, multiple colonization events, supplying species that are functionally redundant under different conditions, may be required. Depending on dispersal rates, and the diversity and composition of regional species pools, this may be unlikely or even impossible. At Portal, dispersal limitation introduced a 20-year delay in the compensatory response driven by *C. baileyi*. Theoretically, a new species capable of compensating for kangaroo rats, and better-suited to conditions at the site since 2010, could restore compensation under present conditions – but it is unclear whether this species exists or if it can disperse to this site. As ecosystems globally undergo reductions in habitat connectivity

and regional beta diversity, and enter novel climatic spaces, maintenance of community function via functional redundancy may grow increasingly rare and fragile [15, 74].

Finally, the long-term variability in functional redundancy documented here adds important nuance to our understanding of how zero-sum dynamics operate in natural assemblages. Theories invoking zero-sum dynamics, and tests for compensatory dynamics in empirical data, often treat a zero-sum dynamic as a strong and temporally consistent constraint [34, 33]. In this framing, any resources made available via species loss should immediately be taken up by other species. This is not consistent with the dynamics that occur at Portal, which has seen extended periods of time when resources are available on exclosure plots but are not used. Rather, these results are more consistent with a zero-sum constraint operating at metacommunity or evolutionary scales [67, 63, 42]. Over short timescales, or within a closed local assemblage, niche differences may weaken zero-sum effects, especially under fluctuating conditions. However, over larger temporal and spatial scales, dispersal or evolution may supply new species equipped to use available resources - via either functional redundancy, or niche complementarity allowing them to exploit novel niches. A long-term, metacommunity, and even macroevolutionary approach may be necessary to fully understand how zero-sum constraints, functional redundancy, and niche complementarity contribute to the maintenance of community-level function in the face of species extinctions and changing conditions over time.

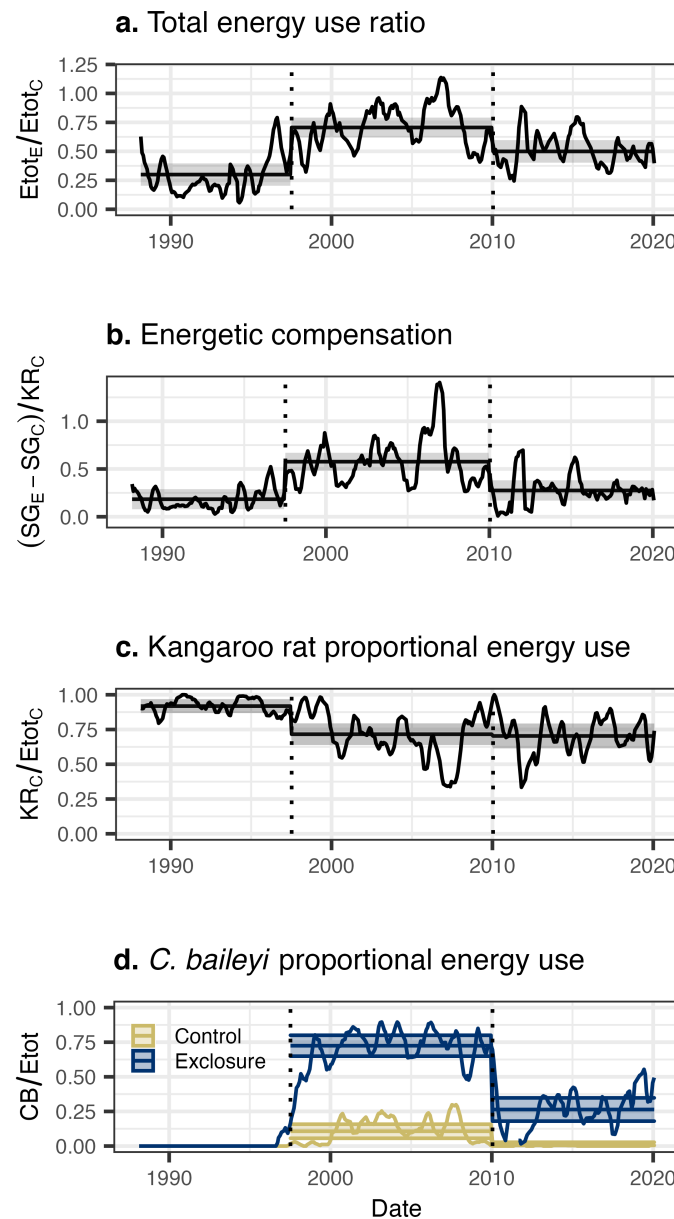


Figure 2-1. Dynamics of energy use and rodent community composition over time. Lines represent the ratio of total energy use on exclosure plots to control plots (a), 6-month moving averages of energetic compensation (b), and the share of community energy use accounted for by kangaroo rats on control plots (c), and by *C. baileyi* (d), on control (gold) and exclosure (blue) plots. Dotted vertical lines mark the boundaries between time periods used for statistical analysis. Horizontal lines are time-period estimates from generalized least squares (a, b) and generalized linear (c, d) models, and the semitransparent envelopes mark the 95% confidence or credible intervals.

CHAPTER 3

TEMPORAL CHANGES IN THE INDIVIDUAL SIZE DISTRIBUTION DECOUPLE LONG-TERM TRENDS IN ABUNDANCE, BIOMASS, AND ENERGY USE OF NORTH AMERICAN BREEDING BIRD COMMUNITIES

3.1 Background

Understanding the interrelated dynamics of size- and individuals-based dimensions of biological abundance is key to understanding trends in biodiversity in the Anthropocene. Total individual abundance - i.e. the total number of individual organisms present in a system - and size-based currencies, such as the total biomass or total metabolic flux (“energy use”) of a system, are intertwined, but nonequivalent, measures of biological function. Abundance is most closely tied to species-level population dynamics, while size-based metrics more directly reflect assemblage-level resource use and contributions to materials fluxes at the broader ecosystem scale [49, 16, 10, 73]. While these currencies are naturally linked [49, 30], changes in size composition can decouple the dynamics of one currency from another [21, 16, 72, 73, 76]. This can mean that intuition from one currency may be misleading about others; a trend in numerical abundance might mask contrasting dynamics occurring with respect to biomass or total energy use [72]. Changes in size composition strong enough to decouple currencies may be symptomatic of important changes in ecosystem status - e.g. abundance-biomass comparison curves in the aquatic realm [53] or size-biased extinctions [77, 61]. In the Anthropocene, as ecosystems globally undergo unprecedented levels of ecological and functional change [24], it is especially important to understand long-term trends in individual abundance, total biomass, total energy use, and the relationship between these currencies.

At the community scale, changes in the relationship between size and abundance can signal important shifts in community structure and functional composition. To the extent that size is a proxy for other functional traits, changes or consistency in the community-level size structure (individual size distribution, ISD) over time may reflect processes related to niche structure [73, 53]. Strong size shifts can decouple the relationship between abundance and biomass. This is especially well-established in aquatic systems, where such changes in the scaling between abundance and biomass often signal ecosystem degradation [70, 39, 53]. Compensatory shifts in the size structure can buffer community function (in terms of biomass or energy use) against

changes in abundance [21, 72, 63]. Or, consistency in the size structure may maintain the relationship between size- and -abundance based currencies, even as species composition, total abundance, and total biomass and total energy use fluctuate over time, which can reflect consistency in the niche structure over time [32]. In contrast to terrestrial trees and aquatic systems, which have received considerable attention in this regard [39, 73], the relationships between community structure, total biomass, and individual abundance remain relatively unknown for terrestrial animals (but see [72]). Terrestrial animal communities exhibit size structure [66, 18], and case studies have demonstrated that size shifts can decouple the dynamics of individual abundance, biomass, and energy use for terrestrial animals [72, 76], but do not always do so [31]. Establishing generalities in these dynamics is especially pertinent in the Anthropocene, as these communities are experiencing extensive and potentially size-structured change, with implications at community, ecosystem, and global scales [77, 59].

Macroecological-scale synthesis on the interrelated dynamics of the ISD, total abundance, and community function for terrestrial animals has been constrained by 1) a lack of community-level size and abundance timeseries data for these systems [66, 73], and 2) appropriate statistical methods for relating change in the size structure to changes in abundance and function [66, 76]. In contrast to aquatic and forest systems, most long-term surveys of animal communities do not collect data on individuals' sizes across a full community (with the exception of small mammal studies, which have made major contributions to our understanding of the dynamics of size, abundance, and function for these systems; [72, 18, 31, 38]). Global, continental, or population-wide studies capture different phenomena [73, 47]. The ISDs for terrestrial animals, and specifically for determinate growing taxa (e.g. mammals, birds), are often complex, multimodal distributions strongly determined by community species composition [32, 66, 18, 76] and less statistically tractable than the power-law ISDs found in aquatic and tree systems [39, 73]. Quantifying change in the size structure, and relating this to change in community-wide abundance and function, is not as straightforward as computing and comparing slopes. As a result, we do not have a general understanding of either 1) how the size structures for

these systems behave over time or 2) the extent to which changes in community size structure decouple the community-level dynamics of abundance, biomass, and energy use in these systems.

Here, we begin to address this gap by exploring how temporal changes in the size structure modulate the relationship between total abundance, energy, and biomass for communities of North American breeding birds. We used allometric scaling to estimate community size and abundance data for the North American Breeding Bird Survey, and evaluated how changes in total abundance, biomass, and energy use have co-varied from 1988-2018. Specifically, we examined: 1) How often do these currencies change together vs. have decoupled dynamics?; 2) What are the dominant directions and magnitudes of the overall change over time and degree of decoupling between the currencies?; 3) To what extent do changes in species composition and community size structure translate into decoupling in the temporal trends of different currencies at the community scale?

3.2 Methods

Code to replicate these analyses is available online at <https://github.com/diazrenata/diss-BBsize> and <https://github.com/diazrenata/invisible-string>.

3.2.1 Bird abundance data

We used data from the Breeding Bird Survey [52] to evaluate trends in abundance, biomass, and energy use. The Breeding Bird Survey consists of roughly 40 kilometer-long survey routes distributed throughout the United States and Canada. Routes are surveyed annually during the breeding season (predominately May-June), via 50 3-minute point counts during which all birds seen or heard are identified to species [52]. Sampling began in 1966, and routes have been added over time to a current total of roughly 3000 routes [52]). We take the route to be the “community” scale [66]. We filtered the Breeding Bird Survey data to remove taxa that are poorly sampled through the point-count methods used in the Breeding Bird Survey, following [28]. We accessed the data, and performed this preliminary cleaning and filtering, using the R package *MATSS* [75].

We explored trends in abundance, biomass, and energy use over the 30-year time period from 1988-2018. We selected these years to provide a temporal window sufficient to detect

long-term trends [11]), while allowing for a substantial number of routes. To avoid irregularities caused by missing time steps, we restricted the main analysis to routes that had been sampled in at least 27 of 31 years in this window ($n = 739$), and compared these results to a more strict selection of routes that were sampled in every year ($n = 199$). Results for this more conservative subset of routes were qualitatively the same as for the more inclusive selection of routes (Appendix B).

3.2.2 Estimated size data

The Breeding Bird Survey contains abundances for all species along a route in each year, but does not include measurements of individual body size. We generated body size estimates for individual birds assuming that intraspecific size distributions are normally distributed around a species' mean body size (following [66]). Using records of species' mean and standard deviation body sizes from [17], we drew individuals' body sizes from the appropriate normal distributions. For species for which there was not a standard deviation recorded in [17] (185 species affected, of 421 total), we estimated the standard deviation using an allometric scaling relationship between mean and standard deviation in body mass based on the records for which the standard deviation was provided. Using these records, we fit a linear model of the form $\log(\text{var}(m)) = \log(\bar{m})$, where m is body mass (model $R^2 = .89$), which yielded the scaling relationship $\text{var}(m) = 0.0047\bar{m}^{2.01}$ (see also [66] for this scaling relationship calculated on a slightly different subset of the Breeding Bird Survey). For species with multiple records in [17], we used the mean \bar{m} and standard deviation of m across all records (averaging across sexes, subspecies, and records from different locations). We performed this averaging after estimating any missing standard deviation measurements.

We simulated individual-level body mass measurements for each individual bird observed by drawing from the normal distribution with the mean and standard deviation of body mass estimated for each bird's species [66]. For each individual bird, we estimated metabolic rate as $10.5(m^{0.713})$ [25, 50, 48]. For each route in each year, we computed total energy use, total biomass, and total abundance by summing over all individuals observed on that route in that year. This method does not incorporate intraspecific variation in body size across geographies or

changes in species' mean body size over time [17, 26]. However, it makes it possible to conduct macroecological studies of avian size distributions at a spatial and temporal scale that would otherwise be impossible [66]. An R package containing code to generate these size estimates is available at <https://github.com/diazrenata/diss-BBSsize>.

3.2.3 Comparing abundance- and size- based currencies

Comparing trends across different currencies is a nontrivial statistical problem. Because different currencies vary widely in their units of measure (e.g. abundance in the hundreds of individuals; total biomass in the thousands of grams), it is challenging to interpret differences in magnitude of slope across different currencies. Transformation and scaling using common approaches (such as a square-root transformation, or rescaling each currency to a mean of 0 and a standard deviation of 1) destroys information about the degree of variability within each currency that is necessary in order to make comparisons between currencies for the same timeseries.

Rather than attempting to compare slopes across currencies or to transform different currencies to a common scale, we used a simple null model to compare the observed dynamics for biomass and energy use to the dynamics that would occur in a scenario in which the species composition (and therefore, in this context, size structure) of the community was consistent throughout the timeseries, but in which total individual abundance varied over time consistent with the observed dynamics. For each route, we characterized the “observed” timeseries of total biomass and total energy use by simulating size measurements for all individuals observed in each time step and summing across individuals, using the method described above. We then simulated timeseries for “individuals-driven” dynamics of biomass and energy use incorporating observed changes in community-wide individual abundance over time, but under a scenario of consistent species (and therefore approximate size) composition over time. For each community, we characterized the timeseries-wide probability of an individual drawn at random from the community belonging to a particular species ($P(s_i)$) as each species' mean relative abundance taken across all timesteps:

$$P(s_i) = \frac{\sum_t^T \frac{n_{i,t}}{N_T}}{T}$$

where $n_{i,t}$ is the abundance of species i in timestep t , N_t is the total abundance of all species in timestep t , and T is the total number of timesteps. For each timestep t , we randomly assigned species' identities to the total number of individuals (of all species) observed in that time step (N_t) by drawing with replacement from a multinomial distribution with probabilities weighted according to $P(s)$ for all species. We then simulated body size measurements for individuals, and calculated total energy use and total biomass, following the same procedure as for the observed community. This characterizes the dynamics for size-based currencies expected if the species (and size) composition of the community did not change over time, but incorporating observed fluctuations in total individual abundance. We refer to these dynamics as “individuals-driven” dynamics.

3.2.4 Long-term trends

For each route, we evaluated the 30-year trend in biomass (or energy use) and compared this to the trend derived from the “individuals-driven” null model using generalized linear models with a Gamma family and log link (appropriate for strictly-positive response variables such as biomass or total energy use). We selected between four model formulas, corresponding to qualitatively different “syndromes” of change, to characterize 1) the trend in biomass (or energy use) over time and 2) whether this trend deviates from the trend expected given only changes in individual abundance:

- $\text{biomass} = \text{year} * \text{dynamics}$ or $\text{energy use} = \text{year} * \text{dynamics}$ in which “dynamics” refers to being either the “observed” or “individuals-driven” (null model) dynamics. This model fits a slope and intercept for the observed trend in biomass or energy use over time, and a separate slope and intercept for the trend drawn from the individuals-driven dynamics. We refer to this model as describing a syndrome of “Decoupled trends” between individuals-driven and observed dynamics.

- $\text{biomass} = \text{year} + \text{dynamics}$ or $\text{energy use} = \text{year} + \text{dynamics}$. This model fits a separate intercept, but not slope, for the individuals-driven and observed dynamics. This model was never selected as the best-performing description of community dynamics.

- $\text{biomass} = \text{year}$ or $\text{energy use} = \text{year}$. This model fits a temporal trend, but does not fit

separate trends for the observed and individuals-driven dynamics. We refer to this syndrome as “Coupled trends” between individuals-driven and observed dynamics.

- $\text{biomass} = 1$ or $\text{energy use} = 1$. The intercept-only model describes no directional change over time for either the observed or individuals-driven dynamics, and we refer to this syndrome as describing “No directional change” for either type of dynamics.

We selected the best-fitting model for each route using AICc. In instances where multiple models had AICc scores within two AICc units of the best-fitting model, we selected the simplest model within two AICc units of the best score. We used the model predictions from each route’s best-fitting model to characterize the direction and slope of each route’s long term trends for individuals-driven (null) and biomass- or energy use-driven (observed) dynamics. For each route’s best-fitting model, we extracted the predicted values for the first (usually 1988) and last (usually 2018) year sampled, for both the observed and null trajectories. We calculated the magnitude of change over time as the ratio of the last (2018) to the first (1988) value, and characterized the direction of the long-term trend as increasing if this ratio was greater than one, and decreasing if it was less than one.

3.2.5 Relating change in community structure to decoupling between individual- and size-based dynamics

We used dissimilarity metrics to explore the extent to which change in community structure propagates to decoupling between long-term trends in individual abundance and total biomass and energy use. These dissimilarity metrics are most readily interpretable when making pairwise comparisons (as opposed to repeated comparisons over a timeseries). We therefore made comparisons between the first and last five-year intervals in each timeseries, resulting in a “begin” and “end” comparison separated by a relatively consistent window of time across routes (usually 19–20 years). The use of five-year periods corrects for sampling effects [71]), smooths out interannual variability, and, by including a relatively large proportion $\frac{1}{3}$ of the total timeseries, partially mitigates the impact of scenarios where the start and end values do not align with the long-term trend.

We calculated three metrics to explore how changes in community composition and size structure translate into decoupling between individuals-driven and observed dynamics for biomass and energy use. First, we evaluated the change in average community-wide body size, calculated as the absolute log ratio of mean body size in the last five years relative to the mean body size in the first five years: absolute log ratio = $\ln \frac{\bar{m}_{last5}}{\bar{m}_{first5}}$ where \bar{m}_{first5} and \bar{m}_{last5} is the mean body size of all individuals observed in the first and last 5 years, respectively. We used the absolute log ratio in order to focus on the magnitude, rather than the direction, of change in body size (see also [62] for the use of the absolute log ratio to examine the magnitudes of differences between values). Large changes in community-wide average body size are, by mathematical necessity, expected to translate into decoupling between observed and abundance-driven dynamics.

Second, we calculated measures of turnover in the size structure and in species composition. We calculated turnover in the ISD using a measure inspired by an overlap measure that has previously been applied to species body size distributions in mammalian communities [56]. We characterized each “begin” or “end” ISD as a smooth probability density function by fitting a Gaussian mixture model (with up to 15 Gaussians, fit following [66]) to the raw distribution of body masses, and extracting the fitted probability density at 1000 evaluation points corresponding to body masses encompassing and extending beyond the range of body masses present in this dataset (specifically, from 0 to 15 kilograms; mean body masses in this dataset range from 2.65 grams, for the Calliope hummingbird *Selasphorus calliope*, to 8.45 kg, for the California condor *Gymnogyps californianus*). We rescaled each density function such that the total probability density summed to 1. To calculate the degree of turnover between two ISDs, we calculated the area of overlap between the two density smooths as

ISD turnover = $\sum \min(density1_i, density2_i)$ where $density1_i$ is the probability density from the density smooth for the first ISD at evaluation point i , and $density2_i$ is the probability density from the density smooth for the second ISD at that evaluation point. We subtracted this quantity from 1 to obtain a measure of turnover between two ISDs.

To evaluate turnover in species composition between the five-year time periods, we

calculated Bray-Curtis dissimilarity between the two communities using the R package *vegan* [54].

We tested whether routes whose dynamics were best-described by each “syndrome” of change – i.e. “Decoupled trends”, “Coupled trends”, or “No directional change” – differed in 1) the magnitude of change in mean body size; 2) turnover in the ISD over time; or 3) species compositional turnover (Bray-Curtis dissimilarity) over time. For change in mean body size, we fit an ordinary linear model of the form *absolute log ratio = syndrome*. We compared this model to an intercept-only null model of the *absolute log ratio = 1*. Because our metrics for turnover in the ISD and species composition are bounded from 0-1, we analyzed these metrics using binomial generalized linear models of the form *ISD turnover = syndrome* and *Bray Curtis dissimilarity = syndrome*, and again compared these models to intercept-only null models. In instances where the model fit with a term for syndrome outperformed the intercept-only model, we calculated model estimates and contrasts using the R package *emmeans* [43].

3.3 Results

Of the 739 routes in this analysis, approximately 70% (500/739 for biomass, and 509/739 for energy use) exhibited syndromes of “Decoupled trends” or “Coupled trends” (that is, were best-described using a model incorporating a temporal trend in individuals-driven and/or biomass or energy use-driven dynamics (Table 3-1)). All results were qualitatively the same using a subset of 199 routes with complete temporal sampling over time (Appendix B). Trends driven by individual abundance, as reflected by the dynamics of a simple null model, were strongly dominated by declines (335 decreases and 165 increases for individuals-driven dynamics in biomass, and 355 decreases and 154 increases for individuals-driven dynamics in energy use; Figure 3-2; Table 3-2). However, for biomass, the long-term temporal trends were evenly balanced between increases and decreases (256 decreasing trends, and 244 increasing trends; Figure 3-2; Table 3-2). For energy use, there was a greater representation of decreasing trends than for biomass, but still less so than for strictly abundance-driven dynamics (329 decreasing trends and 180 increasing trends; Figure 3-2; Table 3-2).

These divergent aggregate outcomes in individual abundance, energy use, and especially biomass occurred due to decoupling in the long-term trends for these different currencies. For a substantial minority of routes (20% of all routes for biomass, and 7% of all routes for energy use), long-term dynamics were best-described as a syndrome of “Decoupled trends” (that is, with a different slope for biomass or energy use-driven dynamics than for the “null”, individuals-driven, trend) (Table 3-1). When this decoupling occurred, it was dominated by instances in which the slope for individuals-driven dynamics was more negative than that for biomass or energy use (Figure 3-3).

Decoupling between the long-term trajectories of individual abundance and energy use or biomass is, by definition, indicative of some degree of change in the community size structure over time. Routes whose dynamics for biomass were best-described as syndromes of decoupled trends over time had a higher absolute log ratio of mean mass (i.e. greater magnitude of change, either increasing or decreasing, in mean mass over time) than routes with coupled or no directional trends (Figure 3-4; Appendix B). However, there was not a detectable difference in the degree of temporal turnover in the ISD overall (Figure 3-4; Appendix B), or in species composition (Figure 3-4; Appendix B), compared between routes that exhibited different syndromes of change.

3.4 Discussion

3.4.1 Abundance, biomass, and energy use are nonequivalent currencies

Simultaneously examining multiple currencies of community-level abundance revealed qualitatively different continent-wide patterns in the long-term trends for the number of individuals, total biomass, and energy use. While long-term trends in individual abundance were dominated by decreases, long-term trends in biomass were evenly split between increases and decreases, and trends in energy use were again dominated by declines (Figure 3-2). These different currencies, though intrinsically linked, describe nonequivalent dimensions of community function and reflect different classes of structuring processes [49]. Individual abundance is most directly linked to species-level population dynamics of the type often considered in classic,

particularly theoretical, approaches to studying competition, compensation, and coexistence (e.g. [34, 7]). Biomass most directly reflects the productivity of a community and its potential contributions to materials fluxes in the broader ecosystem context, whereas energy use - by taking into account the metabolic inefficiencies of organisms of different body size - characterizes the total resource use of a community and may come the closest to capturing signals of bottom-up constraints, “Red Queen” effects, or zero-sum competitive dynamics [67, 20, 21, 49, 72]. Our results underscore that, while trends in individual abundance, biomass, and energy use naturally co-vary to some extent, shifts in the community size structure can and do produce qualitatively different trends for these different currencies. These may reflect contrasting long-term changes in different types of community processes - for example, shifts in habitat structure that affect the optimal body sizes for organisms in a system, but do not result in overall changes in resource availability (e.g. [72]). Moreover, extrapolating the long-term trend from one currency to another may mask underlying changes in the community that complicate these dynamics. To appropriately monitor different dimensions of biodiversity change, it is therefore important to focus on the specific currency most closely aligned with the types of processes and dynamics - e.g. population fluctuations, resource limitation, or materials fluxes - of interest in a particular context.

3.4.2 For North American breeding birds, biomass has declined less than abundance or energy use

For communities with a decoupling in the long-term trends of biomass, energy use, and abundance, this decoupling is indicative of a directional shift in the size structure of the community. For the communities of breeding birds across North America considered here, the long-term trends in total biomass are often less negative than trends in total individual abundance or total energy use (Figure 3). This consistent (but not ubiquitous) signal corresponds to community-level increases in average body size that partially or completely buffer changes in total biomass against declines in the overall number of individuals. This contrasts with taxonomically general, global concerns that larger-bodied species are more vulnerable to extinction and population declines than smaller ones [77, 14, 61]. However, it is consistent with

previous findings from the Breeding Bird Survey [58]. The long-term trends for communities of different taxonomic groups, geographies, or temporal spans may show different effects related to different facets of global change and biodiversity responses. We also note that these increases in body size do not generally appear great enough to decouple the long-term trends in energy use from total individual abundance (Figure 3-3). Energy use scales nonlinearly with body size with an exponent less than 1, which means that community-wide increases in mean body size result in smaller increases in total energy use than in total biomass.

3.4.3 Complex relationships between compositional change and community-level properties

The decoupling between the long-term trends for biomass, individual abundance, and energy use demonstrated in many of the communities studied here is symptomatic of a directional shift in the size structure - in these instances, generally favoring larger bodied species. However, examining the community-wide dynamics of turnover in species composition and the overall size structure reveals that the relationship between changes in community structure and changes in the scaling between different currencies of community-wide abundance is considerably more nuanced than simple directional shifts in mean size. Routes that exhibit a statistically detectable decoupling between total biomass and total abundance show large changes in average body size compared to routes for which biomass and abundance either change more nearly in concert with each other or do not show temporal trends (Figure 3-4; Appendix B). This aligns naturally with mathematical intuition given the intrinsic relationship between average body size, total abundance, and total biomass. However, these routes are not extraordinary in terms of their overall degree of temporal turnover in either the size structure or in species composition. Rather, the levels of turnover in overall community size structure and species composition are comparable between routes that show decoupling between abundance and biomass, statistically indistinguishable trends, or no temporal trends in either currency (Figure 3-4; Appendix B).

For many communities, therefore, there has been appreciable change in species and size composition that does not manifest in a shift in the overall community-wide mean body size or

mean metabolic rate sufficient to decouple the dynamics of biomass, abundance, and energy use. These changes may signal changes in functional composition equally important as the ones that manifest in directional shifts in community-wide average body size. For the complex, multimodal size distributions that are the norm for avian communities [66], changes in the number and position of modes may be as important as changes in higher-level statistical moments such as the overall mean. At present, the field lacks the statistical tools and conceptual frameworks to quantify and interpret these nuanced changes, especially at the macroecological scale of the current study [66, 76]. However, this is an excellent opportunity for more system-specific work, informed by natural history knowledge and process-driven expectation, to characterize more nuanced changes in the size structure of specific communities and identify the underlying drivers of these changes. To facilitate these efforts in the context of the Breeding Bird Survey, the R package we have developed to characterize the individual size distributions for avian communities based on species' identities and/or mean body sizes is freely available for re-use and wider applications (<https://github.com/diazrenata/diss-BBSize>; the general-use version of this package is currently in development at <https://github.com/diazrenata/birdsize>).

3.4.4 Conclusion

This analysis demonstrates the current power, and limitations, of a data-driven macroecological perspective on the interrelated dynamics of community size structure and different dimensions of community-wide abundance for terrestrial animal communities. For breeding bird communities across North America, we find that changes in species and size composition produce qualitatively different aggregate patterns in the long-term trends of abundance, biomass, and energy use, highlighting the nuanced relationship between these related, but decidedly nonequivalent, currencies and reflecting widespread changes in community size structure that may signal substantive changes in functional composition. Simultaneously, the complex relationship between turnover in community species and size composition, and the scaling between different currencies of community-level abundance, highlights opportunities for synergies between recent computational and statistical advances, case studies grounded in

empiricism and natural history, and future macroecological-scale synthesis to realize the full potential of this conceptual space.

CHAPTER 4

EXAMPLES OF EDITOR/AUTHOR TOOLS, TABLES, AND IMAGES

4.1 Example of using the authorRemark and editorRemark

If you don't see any blue or red type under this line, then you almost certainly need to include the optional "editMode" to the document class. Thus your document class (first line) should read \documentclass[editMode]{ufdissertation}.

Test! This is a remark written by the author, to themselves, for review purposes. It will be suppressed unless editMode is used in the class options.

This is an editor's remark, written by an editor in-line so that they can write into the content itself with something easy to see. But the remark will be suppressed unless editMode is used in the class options.

To get this remark to go away, simply remove "editMode" from the documentclass options at the top of the user's tex-file. This also removes the blue Author Remarks.

4.2 Table Examples

You may notice that some tables get moved outside of where you placed them. This is because L^AT_EX is a little too helpful when it comes to placement of 'float' types; which includes tables and figures. You can get around this by using the "H" parameter in the table environment, or the 'multiFigure' environment described in the "adding graphics section"; ie section 4.4

Table 4-1. This table is located in the correct section because it uses the "H" optional parameter in the table environment, unlike the next tables which have been helpfully moved by L^AT_EX to the next page, which places them inside the section. You should also make a note that the caption command is placed after the table itself, which means the caption occurs after the table. The graduate school requires tables to have captions placed before the actual table data, so the caption command should be located before the table data. See the next table for an example.

Some	Data	Goes	Here
Some	Data	Goes	Here
Some	Data	Goes	Here
Some	Data	Goes	Here

4.3 Very Long Tables

There are two approaches to inputting very long tables. You can do it manually, or you can do it using the longtables package. Here we include an example of both. Table 4-3 is done manually, whereas 4-4 is done using the longtables package.

Table 4-2. Notice that this caption is included above the table data, as per the graduate school requirements. Also note that the caption itself has a short version in the “List of Tables” which is achieved by using the optional argument of the caption command. See the file source code directly to see the example. Unfortunately, since we did not use the “H” parameter in the table environment, this table was placed *after* the next section heading, which is almost certainly not where an author would have wanted it.

Some	Data	Goes	Here
Some	Data	Goes	Here
Some	Data	Goes	Here
Some	Data	Goes	Here

Table 4-3. Feasible triples for highly variable Grid, MLMMH.

Time (s)	Triple chosen	Other feasible triples
0	(1, 11, 13725)	(1, 12, 10980), (1, 13, 8235), (2, 2, 0), (3, 1, 0)
2745	(1, 12, 10980)	(1, 13, 8235), (2, 2, 0), (2, 3, 0), (3, 1, 0)
5490	(1, 12, 13725)	(2, 2, 2745), (2, 3, 0), (3, 1, 0)
8235	(1, 12, 16470)	(1, 13, 13725), (2, 2, 2745), (2, 3, 0), (3, 1, 0)
10980	(1, 12, 16470)	(1, 13, 13725), (2, 2, 2745), (2, 3, 0), (3, 1, 0)
13725	(1, 12, 16470)	(1, 13, 13725), (2, 2, 2745), (2, 3, 0), (3, 1, 0)
16470	(1, 13, 16470)	(2, 2, 2745), (2, 3, 0), (3, 1, 0)
19215	(1, 12, 16470)	(1, 13, 13725), (2, 2, 2745), (2, 3, 0), (3, 1, 0)
21960	(1, 12, 16470)	(1, 13, 13725), (2, 2, 2745), (2, 3, 0), (3, 1, 0)
24705	(1, 12, 16470)	(1, 13, 13725), (2, 2, 2745), (2, 3, 0), (3, 1, 0)
27450	(1, 12, 16470)	(1, 13, 13725), (2, 2, 2745), (2, 3, 0), (3, 1, 0)
30195	(2, 2, 2745)	(2, 3, 0), (3, 1, 0)
32940	(1, 13, 16470)	(2, 2, 2745), (2, 3, 0), (3, 1, 0)
35685	(1, 13, 13725)	(2, 2, 2745), (2, 3, 0), (3, 1, 0)
38430	(1, 13, 10980)	(2, 2, 2745), (2, 3, 0), (3, 1, 0)
41175	(1, 12, 13725)	(1, 13, 10980), (2, 2, 2745), (2, 3, 0), (3, 1, 0)
43920	(1, 13, 10980)	(2, 2, 2745), (2, 3, 0), (3, 1, 0)
46665	(2, 2, 2745)	(2, 3, 0), (3, 1, 0)
49410	(2, 2, 2745)	(2, 3, 0), (3, 1, 0)
52155	(1, 12, 16470)	(1, 13, 13725), (2, 2, 2745), (2, 3, 0), (3, 1, 0)
54900	(1, 13, 13725)	(2, 2, 2745), (2, 3, 0), (3, 1, 0)
57645	(1, 13, 13725)	(2, 2, 2745), (2, 3, 0), (3, 1, 0)
60390	(1, 12, 13725)	(2, 2, 2745), (2, 3, 0), (3, 1, 0)
63135	(1, 13, 16470)	(2, 2, 2745), (2, 3, 0), (3, 1, 0)
65880	(1, 13, 16470)	(2, 2, 2745), (2, 3, 0), (3, 1, 0)
68625	(2, 2, 2745)	(2, 3, 0), (3, 1, 0)
71370	(1, 13, 13725)	(2, 2, 2745), (2, 3, 0), (3, 1, 0)
74115	(1, 12, 13725)	(2, 2, 2745), (2, 3, 0), (3, 1, 0)
76860	(1, 13, 13725)	(2, 2, 2745), (2, 3, 0), (3, 1, 0)
79605	(1, 13, 13725)	(2, 2, 2745), (2, 3, 0), (3, 1, 0)
82350	(1, 12, 13725)	(2, 2, 2745), (2, 3, 0), (3, 1, 0)

Table 4-3. Continued

Time (s)	Triple chosen	Other feasible triples
85095	(1, 12, 13725)	(1, 13, 10980), (2, 2, 2745), (2, 3, 0), (3, 1, 0)
87840	(1, 13, 16470)	(2, 2, 2745), (2, 3, 0), (3, 1, 0)
90585	(1, 13, 16470)	(2, 2, 2745), (2, 3, 0), (3, 1, 0)
93330	(1, 13, 13725)	(2, 2, 2745), (2, 3, 0), (3, 1, 0)
96075	(1, 13, 16470)	(2, 2, 2745), (2, 3, 0), (3, 1, 0)
98820	(1, 13, 16470)	(2, 2, 2745), (2, 3, 0), (3, 1, 0)
101565	(1, 13, 13725)	(2, 2, 2745), (2, 3, 0), (3, 1, 0)
104310	(1, 13, 16470)	(2, 2, 2745), (2, 3, 0), (3, 1, 0)
107055	(1, 13, 13725)	(2, 2, 2745), (2, 3, 0), (3, 1, 0)
109800	(1, 13, 13725)	(2, 2, 2745), (2, 3, 0), (3, 1, 0)
112545	(1, 12, 16470)	(1, 13, 13725), (2, 2, 2745), (2, 3, 0), (3, 1, 0)
115290	(1, 13, 16470)	(2, 2, 2745), (2, 3, 0), (3, 1, 0)
118035	(1, 13, 13725)	(2, 2, 2745), (2, 3, 0), (3, 1, 0)
120780	(1, 13, 16470)	(2, 2, 2745), (2, 3, 0), (3, 1, 0)
123525	(1, 13, 13725)	(2, 2, 2745), (2, 3, 0), (3, 1, 0)
126270	(1, 12, 16470)	(1, 13, 13725), (2, 2, 2745), (2, 3, 0), (3, 1, 0)
129015	(2, 2, 2745)	(2, 3, 0), (3, 1, 0)
131760	(2, 2, 2745)	(2, 3, 0), (3, 1, 0)
134505	(1, 13, 16470)	(2, 2, 2745), (2, 3, 0), (3, 1, 0)
137250	(1, 13, 13725)	(2, 2, 2745), (2, 3, 0), (3, 1, 0)
139995	(2, 2, 2745)	(2, 3, 0), (3, 1, 0)
142740	(2, 2, 2745)	(2, 3, 0), (3, 1, 0)
145485	(1, 12, 16470)	(1, 13, 13725), (2, 2, 2745), (2, 3, 0), (3, 1, 0)
148230	(2, 2, 2745)	(2, 3, 0), (3, 1, 0)
150975	(1, 13, 16470)	(2, 2, 2745), (2, 3, 0), (3, 1, 0)
153720	(1, 12, 13725)	(2, 2, 2745), (2, 3, 0), (3, 1, 0)
156465	(1, 13, 13725)	(2, 2, 2745), (2, 3, 0), (3, 1, 0)
159210	(1, 13, 13725)	(2, 2, 2745), (2, 3, 0), (3, 1, 0)
161955	(1, 13, 16470)	(2, 2, 2745), (2, 3, 0), (3, 1, 0)
164700	(1, 13, 13725)	(2, 2, 2745), (2, 3, 0), (3, 1, 0)

Alternatively, compared to the previous example where we used manual breaks to break the table, we can let LaTeX do this for us, as well as taking care of any recurrent headers and footers, utilizing the `\longtable` command,¹ as follows:

¹note that the `longtable` environment is not in a table environment; putting it inside a table environment will stop it from correctly page breaking as needed.

Table 4-4. Duplicate of Previous table, using longtables environment.

Time (s)	Triple chosen	Other feasible triples
0	(1, 11, 13725)	(1, 12, 10980), (1, 13, 8235), (2, 2, 0), (3, 1, 0)
2745	(1, 12, 10980)	(1, 13, 8235), (2, 2, 0), (2, 3, 0), (3, 1, 0)
5490	(1, 12, 13725)	(2, 2, 2745), (2, 3, 0), (3, 1, 0)
8235	(1, 12, 16470)	(1, 13, 13725), (2, 2, 2745), (2, 3, 0), (3, 1, 0)
10980	(1, 12, 16470)	(1, 13, 13725), (2, 2, 2745), (2, 3, 0), (3, 1, 0)
13725	(1, 12, 16470)	(1, 13, 13725), (2, 2, 2745), (2, 3, 0), (3, 1, 0)
16470	(1, 13, 16470)	(2, 2, 2745), (2, 3, 0), (3, 1, 0)
19215	(1, 12, 16470)	(1, 13, 13725), (2, 2, 2745), (2, 3, 0), (3, 1, 0)
21960	(1, 12, 16470)	(1, 13, 13725), (2, 2, 2745), (2, 3, 0), (3, 1, 0)
24705	(1, 12, 16470)	(1, 13, 13725), (2, 2, 2745), (2, 3, 0), (3, 1, 0)
27450	(1, 12, 16470)	(1, 13, 13725), (2, 2, 2745), (2, 3, 0), (3, 1, 0)
30195	(2, 2, 2745)	(2, 3, 0), (3, 1, 0)
32940	(1, 13, 16470)	(2, 2, 2745), (2, 3, 0), (3, 1, 0)
35685	(1, 13, 13725)	(2, 2, 2745), (2, 3, 0), (3, 1, 0)
38430	(1, 13, 10980)	(2, 2, 2745), (2, 3, 0), (3, 1, 0)
41175	(1, 12, 13725)	(1, 13, 10980), (2, 2, 2745), (2, 3, 0), (3, 1, 0)
43920	(1, 13, 10980)	(2, 2, 2745), (2, 3, 0), (3, 1, 0)
46665	(2, 2, 2745)	(2, 3, 0), (3, 1, 0)
49410	(2, 2, 2745)	(2, 3, 0), (3, 1, 0)
52155	(1, 12, 16470)	(1, 13, 13725), (2, 2, 2745), (2, 3, 0), (3, 1, 0)
54900	(1, 13, 13725)	(2, 2, 2745), (2, 3, 0), (3, 1, 0)
57645	(1, 13, 13725)	(2, 2, 2745), (2, 3, 0), (3, 1, 0)
60390	(1, 12, 13725)	(2, 2, 2745), (2, 3, 0), (3, 1, 0)
63135	(1, 13, 16470)	(2, 2, 2745), (2, 3, 0), (3, 1, 0)
65880	(1, 13, 16470)	(2, 2, 2745), (2, 3, 0), (3, 1, 0)
68625	(2, 2, 2745)	(2, 3, 0), (3, 1, 0)
71370	(1, 13, 13725)	(2, 2, 2745), (2, 3, 0), (3, 1, 0)
74115	(1, 12, 13725)	(2, 2, 2745), (2, 3, 0), (3, 1, 0)
76860	(1, 13, 13725)	(2, 2, 2745), (2, 3, 0), (3, 1, 0)
79605	(1, 13, 13725)	(2, 2, 2745), (2, 3, 0), (3, 1, 0)
82350	(1, 12, 13725)	(2, 2, 2745), (2, 3, 0), (3, 1, 0)
85095	(1, 12, 13725)	(1, 13, 10980), (2, 2, 2745), (2, 3, 0), (3, 1, 0)
87840	(1, 13, 16470)	(2, 2, 2745), (2, 3, 0), (3, 1, 0)
90585	(1, 13, 16470)	(2, 2, 2745), (2, 3, 0), (3, 1, 0)
93330	(1, 13, 13725)	(2, 2, 2745), (2, 3, 0), (3, 1, 0)
96075	(1, 13, 16470)	(2, 2, 2745), (2, 3, 0), (3, 1, 0)
98820	(1, 13, 16470)	(2, 2, 2745), (2, 3, 0), (3, 1, 0)
101565	(1, 13, 13725)	(2, 2, 2745), (2, 3, 0), (3, 1, 0)
104310	(1, 13, 16470)	(2, 2, 2745), (2, 3, 0), (3, 1, 0)
107055	(1, 13, 13725)	(2, 2, 2745), (2, 3, 0), (3, 1, 0)
109800	(1, 13, 13725)	(2, 2, 2745), (2, 3, 0), (3, 1, 0)
112545	(1, 12, 16470)	(1, 13, 13725), (2, 2, 2745), (2, 3, 0), (3, 1, 0)

Table 4-4. Continued

Time (s)	Triple chosen	Other feasible triples
115290	(1, 13, 16470)	(2, 2, 2745), (2, 3, 0), (3, 1, 0)
118035	(1, 13, 13725)	(2, 2, 2745), (2, 3, 0), (3, 1, 0)
120780	(1, 13, 16470)	(2, 2, 2745), (2, 3, 0), (3, 1, 0)
123525	(1, 13, 13725)	(2, 2, 2745), (2, 3, 0), (3, 1, 0)
126270	(1, 12, 16470)	(1, 13, 13725), (2, 2, 2745), (2, 3, 0), (3, 1, 0)
129015	(2, 2, 2745)	(2, 3, 0), (3, 1, 0)
131760	(2, 2, 2745)	(2, 3, 0), (3, 1, 0)
134505	(1, 13, 16470)	(2, 2, 2745), (2, 3, 0), (3, 1, 0)
137250	(1, 13, 13725)	(2, 2, 2745), (2, 3, 0), (3, 1, 0)
139995	(2, 2, 2745)	(2, 3, 0), (3, 1, 0)
142740	(2, 2, 2745)	(2, 3, 0), (3, 1, 0)
145485	(1, 12, 16470)	(1, 13, 13725), (2, 2, 2745), (2, 3, 0), (3, 1, 0)
148230	(2, 2, 2745)	(2, 3, 0), (3, 1, 0)
150975	(1, 13, 16470)	(2, 2, 2745), (2, 3, 0), (3, 1, 0)
153720	(1, 12, 13725)	(2, 2, 2745), (2, 3, 0), (3, 1, 0)
156465	(1, 13, 13725)	(2, 2, 2745), (2, 3, 0), (3, 1, 0)
159210	(1, 13, 13725)	(2, 2, 2745), (2, 3, 0), (3, 1, 0)
161955	(1, 13, 16470)	(2, 2, 2745), (2, 3, 0), (3, 1, 0)
164700	(1, 13, 13725)	(2, 2, 2745), (2, 3, 0), (3, 1, 0)

4.4 Examples of Adding Graphics

All of the below code with subfigures A-Z was generated with:

```
\begin{multiFigure}

\addFigure{0.3}{./theworld.png}

\addFigure{0.2}{./theworld.png}

\addFigure{0.4}{./theworld.png}

\addFigure[Z]{0.6}{./theworld.png}

\captionof{figure}[This is a test caption.]{This is a test caption.

This text has the bit for the whole figure. Meanwhile, subfigure A is weird
looking map. Subfigure B is a smaller map. And Subfigure C
is a bigger but still weird looking map.

Moreover, I can override the map, which is why Z is
another weird map that came after map C.}

\end{multiFigure}
```

Note that L^AT_EX can be fickle when it comes to placing figures relative to text near the figure. Specifically, the “Figure” environment is a ‘float’ type, which is placed somewhere “nearby” where it appears in the text, which can be pretty frustrating. For this reason we have circumvented the ‘float’ part of the figure in order to allow more control over the figure placement.

If one uses the `\begin{figure}\end{figure}` construction, the figure may appear in a odd place, whereas you can use the `\begin{multiFigure}\end{multiFigure}` even with only 1 figure, to force placement to work. When using multiFigure captions need to be placed using the command `\captionof{<NAME>} [<LIST-ENTRY>] {<CAPTION>}` where NAME is the type of caption, LIST-ENTRY is what appears in the ‘List of’ at the beginning of the thesis, and CAPTION is the actual caption. For single image figures, it will be better to use the `\begin{figure}\end{figure}` construction was the Graduate Editorial Office does not need a letter-label, for a figure with only one image.

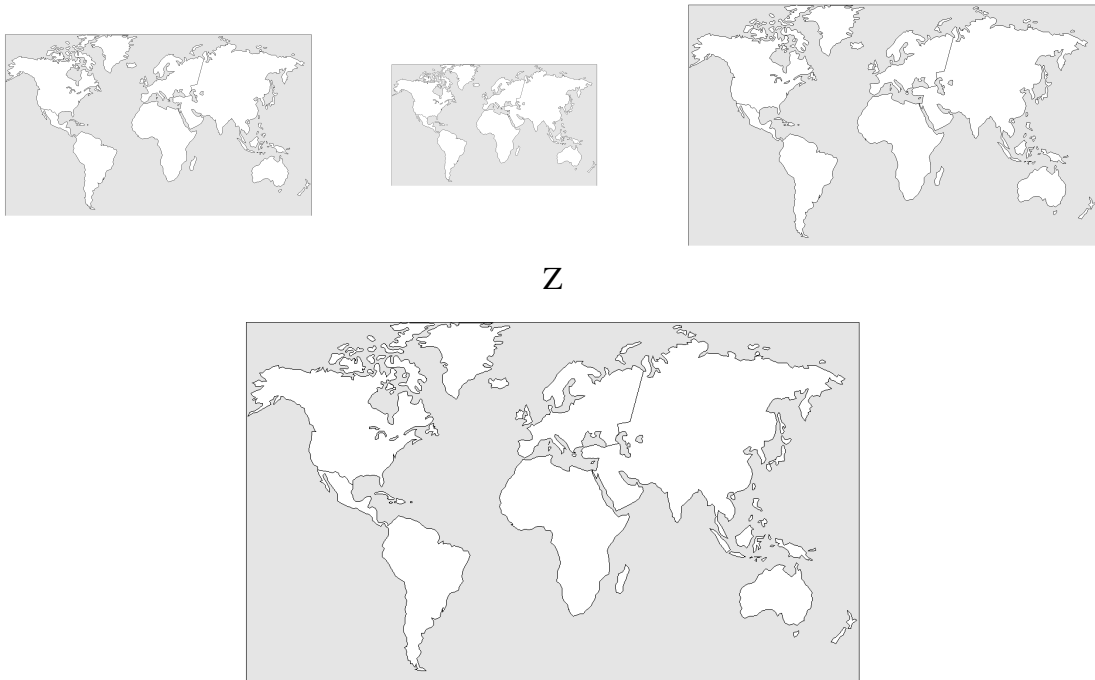


Figure 4-1. This is a test caption. This text has the bit for the whole figure. Meanwhile, subfigure A is weird looking map. Subfigure B is a smaller map. And Subfigure C is a bigger but still weird looking map. Moreover, I can override the map, which is why Z is another weird map that came after map C.



Figure 4-2. This is a super-long caption to make sure that the caption in the list-of-section is correctly single space with the blank white line between captions. That being said, you should probably always use the list-entry optional argument in the captionof command to write a shorter caption instead of this nonsense.

4.5 A Note on Graphics

The command `\addFigure` in the `multiFigure` environment, and/or the command `\includegraphics` will take almost every type of graphic file currently in use as of the writing of this template. The only notable exception is the bitmap, ie `.bmp` file. Most software won't save to bitmap without specifically requesting it at this point, but if you have generated a `.bmp` file you can load it in most any graphic editor (eg MSpaint or photoshop) and save it as a different file type, such as `.PNG` which is significantly smaller file size as well. Note that the commands typically require the file extension to be included, and it is case sensitive. Thus in the above `\addFigure{0.2}{./theworld.png}` works but `\addFigure{0.2}{./theworld.PNG}` would error and `\addFigure{0.2}{./theworld}` may or may not work depending on which specific TeX editor you are using.

4.6 Placement Specifiers

Floats are used to allow LaTeX to handle figures while maintaining the best possible presentation. However, there may be times when you disagree, and a typical example is with its positioning of figures. The placement specifier parameter exists as a compromise, and its purpose is to give the author a greater degree of control over where certain floats are placed.

Table 4-5. Specifier Table

Specifier	Permission
h	Place the float here, i.e., approximately at the same point it occurs in the source text (however, not exactly at the spot)
t	Position at the top of the page.
b	Position at the bottom of the page.
p	Put on a special page for floats only.
!	Override internal parameters LaTeX uses for determining "good" float positions.
H	Places the float at precisely the location in the LaTeX code.

An example of a specifier parameter is shown below to force a figure into place where it is mentioned in text:

```
\begin{figure}[h!]
    \begin{center}
        \includegraphics[width=0.9\textwidth]{./theworld.png}
    \end{center}
    \caption[My short caption.]{My full caption in curly brackets.}
\end{figure}
```

CHAPTER 5

SUMMARY AND CONCLUSIONS

5.1 Non Porttitor Tellus

Aliquam molestie sed urna quis convallis. Aenean nibh eros, aliquam non eros in, tempus lacinia justo. In magna sapien, blandit a faucibus ac, scelerisque nec purus. Praesent fermentum felis nec massa interdum, vel dapibus mi luctus. Cras id fringilla mauris. Ut molestie eros mi, ut hendrerit nulla tempor et. Pellentesque tortor quam, mattis a scelerisque nec, euismod et odio. Mauris rhoncus metus sit amet risus mattis, eu mattis sem interdum.

5.1.1 Nam Arcu Magna

Semper vel lorem eu, venenatis ultrices est. Nam aliquet ut erat ac scelerisque. Maecenas ut molestie mi. Phasellus ipsum magna, sollicitudin eu ipsum quis, imperdiet cursus turpis. Etiam pretium enim a fermentum accumsan. Morbi vel vehicula enim.

5.1.2 Nam Arcu Magna

Semper vel lorem eu, venenatis ultrices est. Nam aliquet ut erat ac scelerisque. Maecenas ut molestie mi. Phasellus ipsum magna, sollicitudin eu ipsum quis, imperdiet cursus turpis. Etiam pretium enim a fermentum accumsan. Morbi vel vehicula enim.

5.1.2.1 Ut pellentesque velit sede

Placerat cursus. Integer congue urna non massa dictum, a pellentesque arcu accumsan. Nulla posuere, elit accumsan eleifend elementum, ipsum massa tristique metus, in ornare neque nisl sed odio. Nullam eget elementum nisi. Duis a consectetur erat, sit amet malesuada sapien. Aliquam nec sapien et leo sagittis porttitor at ut lacus. Vivamus vulputate elit vitae libero condimentum dictum. Nulla facilisi. Quisque non nibh et massa ullamcorper iaculis.[?]

5.1.2.2 Ut pellentesque velit sede

Placerat cursus. Integer congue urna non massa dictum, a pellentesque arcu accumsan. Nulla posuere, elit accumsan eleifend elementum, ipsum massa tristique metus, in ornare neque nisl sed odio. Nullam eget elementum nisi. Duis a consectetur erat, sit amet malesuada sapien. Aliquam nec sapien et leo sagittis porttitor at ut lacus. Vivamus vulputate elit vitae libero condimentum dictum. Nulla facilisi. Quisque non nibh et massa ullamcorper iaculis.[?]

5.2 Non Porttitor Tellus

Aliquam molestie sed urna quis convallis. Aenean nibh eros, aliquam non eros in, tempus lacinia justo. In magna sapien, blandit a faucibus ac, scelerisque nec purus. Praesent fermentum felis nec massa interdum, vel dapibus mi luctus. Cras id fringilla mauris. Ut molestie eros mi, ut hendrerit nulla tempor et. Pellentesque tortor quam, mattis a scelerisque nec, euismod et odio. Mauris rhoncus metus sit amet risus mattis, eu mattis sem interdum.

APPENDIX A SUPPLEMENTAL RESULTS AND ANALYSES FOR CHAPTER 2

A.1 Plot-level analysis

A.1.1 Explanation

In order to calculate energetic compensation and the total energy ratio, we require an estimate for the baseline values of total energy use, kangaroo rat energy use, and small granivore energy use on control plots. Estimating these baselines requires aggregating over between-plot variability among the control plots. For consistency, in the main analysis, we also aggregate across the enclosure plots and focus on treatment-level means throughout. Here, we explore the effect of between-plot variability on our analyses, to the extent possible. We used treatment-level means across control plots to calculate energetic compensation and the total energy ratio, but calculated these quantities separately for each enclosure plot, and conducted analyses including a random effect of plot. We also conducted analyses of *Dipodomys* and *C. baileyi* proportional energy use using plot-level data, again including plot as a random effect. Results were qualitatively the same as using treatment-level means.

A.1.2 Compensation

We fit linear mixed-effects models (using the *lme* function in the R package *nlme*; [54]) of the form $\text{compensation} = \text{timeperiod}$ with a random effect of plot and temporal autocorrelation structure to account for autocorrelation between monthly census periods within each time period. We compared these to models without the autocorrelation structure, without the random effect, and without the term for time period. The best-fitting model included terms for time period, random effect of plot, and autocorrelation.

A.1.3 Total energy use

As for compensation, we fit linear mixed-effects models fitting $\text{totalenergyratio} = \text{timeperiod}$ with a random effect of plot and a temporal autocorrelation term to account for autocorrelation between monthly census periods within each time period. We compared these to models without the autocorrelation term, without the random effect, and without the term for time period. The best-fitting model included terms for time period, random effect of plot, and autocorrelation.

A.1.4 *Dipodomys* proportional energy use

To compare proportional energy use across time periods, we used binomial generalized linear mixed models (using the `glmer` function in the R package `lme4`; Bates (2015)), which allowed us to include a random effect of plot.

For *Dipodomys* proportional energy use, we compared models with and without the random effect of plot and with and without a term for `timeperiod`. The best-fitting model included terms for `timeperiod` and a random effect of plot.

A.1.5 *C. baileyi* proportional energy use

As for kangaroo rat proportional energy use, we used a binomial generalized linear mixed effects model to compare *C. baileyi* proportional energy use across time periods. Because *C. baileyi* occurs on both control and exclosure plots, we investigated whether the dynamics of *C. baileyi*'s proportional energy use differed between treatment types. We compared models incorporating separate slopes, separate intercepts, or no terms for treatment modulating the change in *C. baileyi* proportional energy use across time periods, i.e. comparing the full set of models:

- *c baileyi proportional energy use = timeperiod + treatment + timeperiod:treatment*

-*c baileyi proportional energy use = 1*

- *c baileyi proportional energy use = timeperiod* We also tested a null (intercept-only) model of no change across time periods:

- *c baileyi proportional energy use = 1*

We compared all of these models with and without a random effect of plot. We found that the best-fitting model incorporated a random effect of plot, and fixed effects for time period and for treatment, but no interaction between them (*c baileyi proportional energy use = 1*). We therefore proceeded with this model.

A.1.6 Tables

Table A-1. Plot-level: Model comparison for compensation.

Model specification	AIC
intercept + timeperiod + plot (random effect) + autocorrelation	1360.207
intercept + timeperiod + plot (random effect)	1680.916
intercept + timeperiod + autocorrelation	1409.830
intercept + plot (random effect) + autocorrelation	1408.362
intercept + plot (random effect)	1879.126
intercept	2036.371

Table A-2. Plot-level: Coefficients from linear mixed-effects model for compensation.

	Value	Std.Error	DF	t-value	p-value
(Intercept)	0.3451282	0.1048354	1362	3.292096	0.0010199
oera.L	0.0653090	0.0373313	1362	1.749446	0.0804392
oera.Q	-0.2845830	0.0341063	1362	-8.343990	0.0000000

Table A-3. Plot-level: Estimates from linear mixed-effects model for compensation.

Timeperiod	emmean	SE	df	lower.CL	upper.CL
1988-1997	0.1827673	0.1091842	3	-0.1647055	0.5302400
1997-2010	0.5774892	0.1078860	3	0.2341478	0.9208306
2010-2020	0.2751282	0.1093969	3	-0.0730215	0.6232779

Table A-4. Plot-level: Contrasts from linear mixed-effects model for compensation.

Comparison	estimate	SE	df	t.ratio	p.value
1988-1997 -	-0.3947220	0.0491845	1362	-8.025330	0.0000
1997-2010					
1988-1997 -	-0.0923609	0.0527944	1362	-1.749446	0.1873
2010-2020					
1997-2010 -	0.3023610	0.0496411	1362	6.090948	0.0000
2010-2020					

Table A-5. Plot-level: Model comparison for total energy use.

Model specification	AIC
intercept + timeperiod + plot (random effect) + autocorrelation	474.8558
intercept + timeperiod + plot (random effect)	924.1830
intercept + timeperiod + autocorrelation	507.7842
intercept + plot (random effect) + autocorrelation	543.5425
intercept + plot (random effect)	1266.2097
intercept	1382.7469

Table A-6. Plot-level: Coefficients from linear mixed-effects model for total energy ratio.

	Value	Std.Error	DF	t-value	p-value
(Intercept)	0.5018200	0.0709701	1362	7.070865	0.0e+00
oera.L	0.1454309	0.0301324	1362	4.826392	1.5e-06
oera.Q	-0.2545852	0.0273660	1362	-9.302977	0.0e+00

Table A-7. Plot-level: Estimates from linear mixed-effects model for total energy ratio.

Timeperiod	emmean	SE	df	lower.CL	upper.CL
1988-1997	0.2950508	0.0751321	3	0.0559470	0.5341547
1997-2010	0.7096879	0.0738511	3	0.4746606	0.9447151
2010-2020	0.5007212	0.0752881	3	0.2611207	0.7403216

Table A-8. Plot-level: Contrasts from linear mixed-effects model for total energy ratio.

Comparison	estimate	SE	df	t.ratio	p.value
1988-1997 -	-0.4146370	0.0395736	1362	-10.477622	0.0e+00
1997-2010					
1988-1997 -	-0.2056703	0.0426137	1362	-4.826392	4.6e-06
2010-2020					
1997-2010 -	0.2089667	0.0398571	1362	5.242901	5.0e-07
2010-2020					

Table A-9. Plot-level: Model comparison for kangaroo rat proportional energy use.

Model specification	AIC
intercept + timeperiod + plot (random effect)	1040.861
intercept + plot (random effect)	1162.470
intercept + timeperiod	1108.490
intercept	1208.081

Table A-10. Plot-level: Coefficients from GLMER on kangaroo rat energy use.

	Estimate	Std. Error	z.value	$Pr(> z)$
(Intercept)	2.181163	0.1305753	16.704251	0
oera.L	-1.946096	0.2664545	-7.303670	0
oera.Q	1.124620	0.1769225	6.356572	0

Table A-11. Plot-level: Estimates from GLMER on kangaroo rat energy use.

Timeperiod	prob	SE	df	asympt.LCL	asympt.UCL
1988-1997	0.9823009	0.0062020	Inf	0.9701452	0.9944566
1997-2010	0.7795273	0.0183934	Inf	0.7434769	0.8155777
2010-2020	0.7797464	0.0208516	Inf	0.7388780	0.8206149

Table A-12. Plot-level: Contrasts from GLMER on kangaroo rat energy use.

Comparison	estmimate	SE	df	z.ratio	p.value
1988-1997 -	0.2027736	0.0194108	Inf	10.4464200	0
1997-2010					
1988-1997 -	0.2025545	0.0217545	Inf	9.3109407	0
2010-2020					
1997-2010 -	-0.0002191	0.0278048	Inf	-0.0078811	1
2010-2020					

Table A-13. Plot-level: Model comparison for *C. baileyi* proportional energy use.

Model specification	AIC
intercept + timeperiod + treatment + timeperiod:treatment + plot (random effect)	1021.318
intercept + timeperiod + treatment + plot (random effect)	1020.263
intercept + timeperiod + plot (random effect)	1042.758
intercept + plot (random effect)	1321.149
intercept + timeperiod + treatment + timeperiod:treatment	1166.653
intercept + timeperiod + treatment	1162.901
intercept + timeperiod	1869.097
intercept	2036.489

Table A-14. Plot-level: Coefficients from GLMER on *C. baileyi* energy use.

	Estimate	Std. Error	z.value	$Pr(> z)$
(Intercept)	-2.443643	0.2067789	-11.81766	0
oera.L	-1.866286	0.1530068	-12.19740	0
oera.Q	3.265183	0.2913472	11.20719	0

Table A-15. Plot-level: Estimates from GLMER on *C. baileyi* energy use.

Timeperiod	Treatment	prob	SE	df	asympt.LCL	asympt.UCL
1997-2010	Control	0.0312856	0.0116044	Inf	0.0085414	0.0540297
1997-2010	Exclosure	0.7658194	0.0392864	Inf	0.6888195	0.8428193
2010-2020	Control	0.0023009	0.0008486	Inf	0.0006378	0.0039641
2010-2020	Exclosure	0.1893142	0.0364430	Inf	0.1178872	0.2607412

Table A-16. Plot-level: Contrasts from GLMER on *C. baileyi* energy use.

Comparison	Treatment	estimate	SE	df	z.ratio	p.value
1997-2010	Control	2.639326	0.2163843	Inf	12.1974	0
- 2010-						
2020						
1997-2010	Exclosure	2.639326	0.2163843	Inf	12.1974	0
- 2010-						
2020						

A.2 Full model results

A.2.1 Compensation

We fit a generalized least squares (of the form $\text{compensation} = \text{timeperiod}$; note that “timeperiod” is coded as “oera” throughout) using the *gls* function from the R package *nlme* [54]. Because values from monthly censuses within each time period are subject to temporal autocorrelation, we included a continuous autoregressive temporal autocorrelation structure of order 1 (using the *CORCAR1* function). We compared this model to models fit without the autocorrelation structure and without the time period term using AIC. The model with both the time period term and the autocorrelation structure was the best-fitting model via AIC, and we used this model to calculate estimates and contrasts using the package *emmeans* [43].

A.2.2 Total energy use ratio

As for compensation, we fit a generalized least squares of the form $\text{total energy ratio} = \text{timeperiod}$, accounting for temporal autocorrelation between monthly censuses within each time period using a continuous autoregressive autocorrelation structure of order 1. We compared this model to models fit without the timeperiod term and/or autocorrelation structure, and found the full (timeperiod plus autocorrelation) model had the best performance via AIC. We used this model for estimates and contrasts.

A.2.3 *Dipodomys* proportional energy use

Proportional energy use is bounded 0-1 and cannot be fit with generalized least squares. We therefore used a binomial generalized linear model of the form *Dipodomys proportional energy use = timeperiod*. We compared a model fit with a timeperiod term to an intercept-only (null) model using AIC, and found the timeperiod term improved model fit. We used this model for estimates and contrasts.

Note that we were unable to incorporate temporal autocorrelation into generalized linear models, and we prioritized fitting models of the appropriate family over accounting for autocorrelation. Due to the pronounced differences between time periods for these variables, we were comfortable proceeding without explicitly accounting for autocorrelation.

A.2.4 *C. baileyi* proportional energy use

As for kangaroo rat proportional energy use, we used a binomial generalized linear model to compare *C. baileyi* proportional energy use across time periods. Because *C. baileyi* occurs on both control and exclosure plots, we investigated whether the dynamics of *C. baileyi*'s proportional energy use differed between treatment types. We compared models incorporating separate slopes, separate intercepts, or no terms for treatment modulating the change in *C. baileyi* proportional energy use across time periods, i.e. comparing the full set of models:

- *c baileyi proportional energy use = timeperiod + treatment + timeperiod:treatment*
- *c baileyi proportional energy use = timeperiod + treatment*
- *c baileyi proportional energy use = timeperiod*

We also tested a null (intercept-only) model of no change across time periods:

- *c baileyi proportional energy use = 1*

We found that the best-fitting model incorporated effects for time period and for treatment, but no interaction between them (*c baileyi proportional energy use = timeperiod + treatment*). We therefore proceeded with this model.

A.2.5 Tables

Table A-17. Model comparison for compensation.

Model specification	AIC
intercept + timeperiod + autocorrelation	69.85023
intercept + autocorrelation	84.74902
intercept + timeperiod	157.09726
intercept	252.74534

Table A-18. Coefficients from GLS model for compensation.

	Value	Std.Error	t-value	p-value
(Intercept)	0.3450313	0.0294996	11.696141	0.0000000
oera.L	0.0647933	0.0524103	1.236269	0.2172146
oera.Q	-0.2833553	0.0477359	-5.935890	0.0000000

Table A-19. Estimates from GLS for compensation.

Timeperiod	emmmean	SE	df	lower.CL	upper.CL
1988-1997	0.1835362	0.0520378	44.11081	0.0786683	0.2884041
1997-2010	0.5763899	0.0462641	47.37851	0.4833383	0.6694416
2010-2020	0.2751677	0.0528010	46.75897	0.1689314	0.3814041

Table A-20. Contrasts from GLS for compensation.

Comparison	estimate	SE	df	t.ratio	p.value
1988-1997 -	-0.3928537	0.0689413	47.89422	-5.698378	0.0000
1997-2010					
1988-1997 -	-0.0916315	0.0741194	45.51740	-1.236269	0.4383
2010-2020					
1997-2010 -	0.3012222	0.0694989	49.52957	4.334200	0.0002
2010-2020					

Table A-21. Model comparison for total energy use.

Model specification	AIC
intercept + timeperiod + autocorrelation	-132.92138
intercept + autocorrelation	-118.15000
intercept + timeperiod	13.29396
intercept	156.85988

Table A-22. Coefficients from GLS for total energy ratio.

	Value	Std.Error	t-value	p-value
(Intercept)	0.5016731	0.0271176	18.499880	0.0000000
oera.L	0.1413504	0.0477646	2.959316	0.0033001
oera.Q	-0.2503659	0.0429312	-5.831790	0.0000000

Table A-23. Estimates from GLS for total energy ratio.

Timeperiod	emmmean	SE	df	lower.CL	upper.CL
1988-1997	0.2995118	0.0475806	36.19943	0.2030323	0.3959913
1997-2010	0.7060960	0.0419773	38.51943	0.6211550	0.7910369
2010-2020	0.4994115	0.0480066	37.62774	0.4021956	0.5966274

Table A-24. Contrasts from GLS for total energy ratio.

Comparison	estimate	SE	df	t.ratio	p.value
1988-1997 -	-0.4065842	0.0623398	40.51631	-6.522060	0.0000
1997-2010					
1988-1997 -	-0.1998997	0.0675493	37.12310	-2.959316	0.0144
2010-2020					
1997-2010 -	0.2066845	0.0626456	41.44768	3.299267	0.0056
2010-2020					

Table A-25. Model comparison for kangaroo rat proportional energy use.

Model specification	AIC
intercept + timeperiod	258.3581
intercept	280.8497

Table A-26. Coefficients from GLM on kangaroo rat energy use.

	Estimate	Std. Error	z.value	Pr(> z)
(Intercept)	1.4032480	0.1503201	9.335068	0.0000000
oera.L	-1.1000833	0.2871738	-3.830723	0.0001278
oera.Q	0.5855493	0.2304516	2.540878	0.0110574

Table A-27. Estimates from GLM on kangaroo rat energy use.

Timeperiod	prob	SE	df	asymp.LCL	asymp.UCL
1988-1997	0.9183528	0.0256462	Inf	0.8680872	0.9686183
1997-2010	0.7160901	0.0398537	Inf	0.6379782	0.7942020
2010-2020	0.7035835	0.0456677	Inf	0.6140765	0.7930905

Table A-28. Contrasts from GLM on kangaroo rat energy use.

Comparison	estimate	SE	df	z.ratio	p.value
1988-1997 -	1.4950249	0.3942281	Inf	3.7922836	0.0004
1997-2010					
1988-1997 -	1.5557527	0.4061251	Inf	3.8307227	0.0004
2010-2020					
1997-2010 -	0.0607279	0.2938992	Inf	0.2066282	0.9767
2010-2020					

Table A-29. Model comparison for *C. baileyi* proportional energy use.

Model specification	AIC
intercept + timeperiod + treatment + timeperiod:treatment	237.7643
intercept + timeperiod + treatment	231.0963
intercept + timeperiod	460.8477
intercept	541.3799

Table A-30. Coefficients from GLM on *C. baileyi* energy use.

	Estimate	Std. Error	z.value	Pr(> z)
(Intercept)	-1.574028	0.1670168	-9.424368	0
oera.L	-1.409273	0.2010398	-7.009921	0
oplottotype.L	2.184896	0.2267112	9.637355	0

Table A-31. Estimates from GLM on *C. baileyi* energy use.

Timeperiod	Treatment	prob	SE	df	asympt.LCL	asympt.UCL
1997-2010	Control	0.1069314	0.0258894	Inf	0.0561890	0.1576737
1997-2010	Exclosure	0.7246076	0.0385129	Inf	0.6491236	0.8000915
2010-2020	Control	0.0160560	0.0058224	Inf	0.0046444	0.0274676
2010-2020	Exclosure	0.2639419	0.0428458	Inf	0.1799657	0.3479181

Table A-32. Contrasts from GLM on *C. baileyi* energy use.

Comparison	Treatment	estimate	SE	df	z.ratio	p.value
1997-2010	Control	1.993013	0.2843132	Inf	7.009921	0
- 2010-						
2020						
1997-2010	Exclosure	1.993013	0.2843132	Inf	7.009921	0
- 2010-						
2020						

A.3 Biomass analysis

A.3.1 Compensation

We fit a generalized least squares (of the form $\text{compensation} = \text{timeperiod}$; note that “timeperiod” is coded as “oera” throughout) using the *gls* function from the R package *nlme* [54]. Because values from monthly censuses within each time period are subject to temporal autocorrelation, we included a continuous autoregressive temporal autocorrelation structure of order 1 (using the *CORCAR1* function). We compared this model to models fit without the

autocorrelation structure and without the time period term using AIC. The model with both the time period term and the autocorrelation structure was the best-fitting model via AIC, and we used this model to calculate estimates and contrasts using the package *emmeans* [43].

A.3.2 Total biomass ratio

As for compensation, we fit a generalized least squares of the form $\text{total energy ratio} = \text{timeperiod}$, accounting for temporal autocorrelation between monthly censuses within each time period using a continuous autoregressive autocorrelation structure of order 1. We compared this model to models fit without the timeperiod term and/or autocorrelation structure, and found the full (timeperiod plus autocorrelation) model had the best performance via AIC. We used this model for estimates and contrasts.

A.3.3 *Dipodomys* proportional biomass

Proportional biomass is bounded 0-1 and cannot be fit with generalized least squares. We therefore used a binomial generalized linear model of the form $\text{Dipodomys proportional biomass} = \text{timeperiod}$. We compared a model fit with a timeperiod term to an intercept-only (null) model using AIC, and found the timeperiod term improved model fit. We used this model for estimates and contrasts.

Note that we were unable to incorporate temporal autocorrelation into generalized linear models, and we prioritized fitting models of the appropriate family over accounting for autocorrelation. Due to the pronounced differences between time periods for these variables, we were comfortable proceeding without explicitly accounting for autocorrelation.

A.3.4 *C. baileyi* proportional biomass

As for kangaroo rat proportional biomass, we used a binomial generalized linear model to compare *C. baileyi* proportional biomass across time periods. Because *C. baileyi* occurs on both control and exclosure plots, we investigated whether the dynamics of *C. baileyi*'s proportional biomass differed between treatment types. We compared models incorporating separate slopes, separate intercepts, or no terms for treatment modulating the change in *C. baileyi* proportional biomass across time periods, i.e. comparing the full set of models:

- $c\ baileyi\ proportional\ biomass = timeperiod + treatment + timeperiod:treatment$
- $c\ baileyi\ proportional\ biomass = timeperiod + treatment$
- $c\ baileyi\ proportional\ biomass = timeperiod$ We also tested a null (intercept-only) model

of no change across time periods:

- $c\ baileyi\ proportional\ biomass = 1$

We found that the best-fitting model incorporated effects for time period and for treatment, but no interaction between them ($c\ baileyi\ proportional\ biomass = timeperiod + treatment$). We therefore proceeded with this model.

A.3.5 Tables

Table A-33. Model comparison for compensation.

Model specification	AIC
intercept + timeperiod + autocorrelation	-17.623354
intercept + autocorrelation	-3.297103
intercept + timeperiod	92.184205
intercept	207.804481

Table A-34. Coefficients from GLS model for compensation.

	Value	Std.Error	t-value	p-value
(Intercept)	0.3081443	0.0290539	10.605950	0.0000000
oera.L	0.0711412	0.0514131	1.383719	0.1673549
oera.Q	-0.2799121	0.0465252	-6.016352	0.000000

Table A-35. Estimates from GLS for compensation.

Timeperiod	emmmean	SE	df	lower.CL	upper.CL
1988-1997	0.1435663	0.0511419	39.28312	0.0401458	0.2469867
1997-2010	0.5366915	0.0452745	41.91562	0.4453185	0.6280646
2010-2020	0.2441751	0.0517205	41.17937	0.1397373	0.3486130

Table A-36. Contrasts from GLS for compensation.

Comparison	estimate	SE	df	t.ratio	p.value
1988-1997 -	-0.3931253	0.0673811	43.22895	-5.834358	0.0000
1997-2010					
1988-1997 -	-0.1006089	0.0727090	40.36882	-1.383719	0.3588
2010-2020					
1997-2010 -	0.2925164	0.0678003	44.43055	4.314383	0.0003
2010-2020					

Table A-37. Model comparison for total biomass.

Model specification	AIC
intercept + timeperiod + autocorrelation	-176.57761
intercept + autocorrelation	-162.61339
intercept + timeperiod	-15.98438
intercept	146.61442

Table A-38. Coefficients from GLS for total biomass ratio.

	Value	Std.Error	t-value	p-value
(Intercept)	0.4553971	0.0272418	16.716827	0.0000000
oera.L	0.1454493	0.0477989	3.042941	0.0025257
oera.Q	-0.2531409	0.0427343	-5.923594	0.0000000

Table A-39. Estimates from GLS for total biomass ratio.

Timeperiod	emmean	SE	df	lower.CL	upper.CL
1988-1997	0.2492046	0.0476584	33.82432	0.1523326	0.3460765
1997-2010	0.6620857	0.0419515	35.98516	0.5770030	0.7471684
2010-2020	0.4549009	0.0480215	34.98703	0.3574107	0.5523911

Table A-40. Contrasts from GLS for total biomass ratio.

Comparison	estimate	SE	df	t.ratio	p.value
1988-1997 -	-0.4128811	0.0621739	38.42746	-6.640747	0.0000
1997-2010					
1988-1997 -	-0.2056963	0.0675979	34.67694	-3.042941	0.0121
2010-2020					
1997-2010 -	0.2071848	0.0624325	39.20390	3.318542	0.0054
2010-2020					

Table A-41. Model comparison for kangaroo rat proportional biomass.

Model specification	AIC
intercept + timeperiod	215.2069
intercept	227.9608

Table A-42. Coefficients from GLM on kangaroo rat biomass.

	Estimate	Std. Error	z.value	Pr(> z)
(Intercept)	1.6149566	0.1644937	9.817741	0.0000000
oera.L	-1.1672395	0.3180813	-3.669626	0.0002429
oera.Q	0.6619048	0.2473324	2.676175	0.0074468

Table A-43. Estimates from GLM on kangaroo rat biomass.

Timeperiod	prob	SE	df	asympt.LCL	asympt.UCL
1988-1997	0.9376458	0.0226460	Inf	0.8932605	0.9820310
1997-2010	0.7454543	0.0385025	Inf	0.6699909	0.8209177
2010-2020	0.7426552	0.0437171	Inf	0.6569713	0.8283392

Table A-44. Contrasts from GLM on kangaroo rat biomass.

Comparison	estimate	SE	df	z.ratio	p.value
1988-1997 - 1997-2010	-1.6360275	0.4372643	Inf	3.741508	0.0005
1988-1997 - 2010-2020	-1.6507259	0.4498349	Inf	3.669626	0.0007
1997-2010 - 2010-2020	0.0146984	0.3057707	Inf	0.048070	0.9987

Table A-45. Model comparison for *C. baileyi* proportional biomass.

Model specification	AIC
intercept + timeperiod + treatment + timeperiod:treatment	237.6847
intercept + timeperiod + treatment	231.2374
intercept + timeperiod	466.4937
intercept + treatment	346.2154
intercept	543.7811

Table A-46. Coefficients from GLM on *C. baileyi* biomass.

	Estimate	Std. Error	z.value	Pr(> z)
(Intercept)	-1.538798	0.1671239	-9.207525	0
oera.L	-1.403286	0.2006948	-6.992140	0
oplotype.L	2.270657	0.2298594	9.878462	0

Table A-47. Estimates from GLM on *C. baileyi* biomass.

Timeperiod	Treatment	prob	SE	df	asympt.LCL	asympt.UCL
1997-2010	Control	0.1041331	0.0255800	Inf	0.0539971	0.1542691
1997-2010	Exclosure	0.7425132	0.0376727	Inf	0.6686761	0.8163504
2010-2020	Control	0.0157248	0.0057341	Inf	0.0044861	0.0269634
2010-2020	Exclosure	0.2838438	0.0439192	Inf	0.1977637	0.3699240

Table A-48. Contrasts from GLM on *C. baileyi* biomass.

Comparison	Treatment	estimate	SE	df	z.ratio	p.value
1997-2010	Control	1.984546	0.2838253	Inf	6.99214	0
-	2010-					
2020						
1997-2010	Exclosure	1.984546	0.2838253	Inf	6.99214	0
-	2010-					
2020						

A.4 Covariates of rodent community change

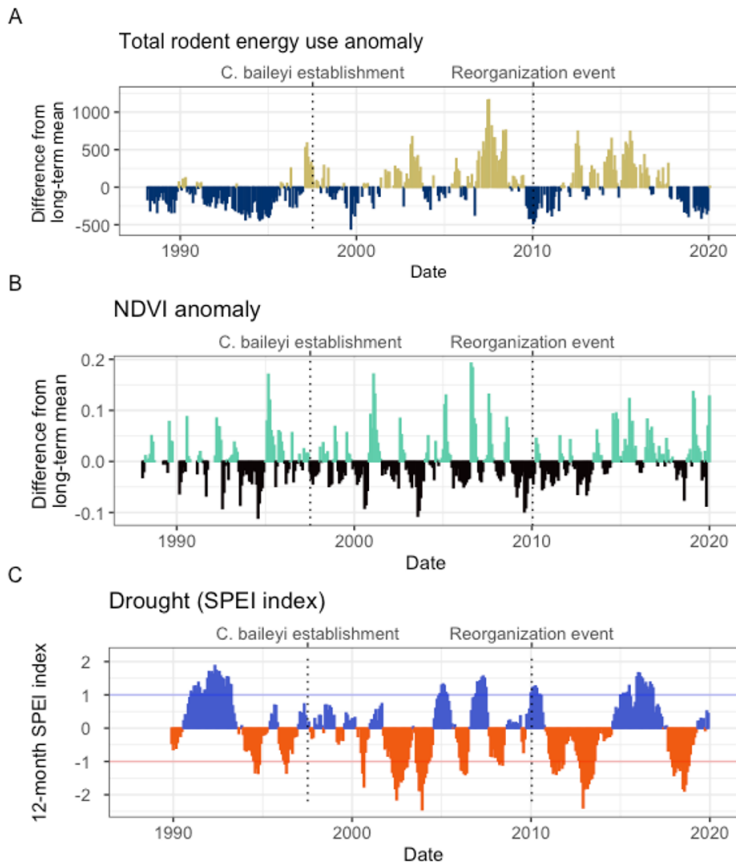


Figure A-1. Changes in overall community energy use (A), NDVI (B), and local climate (C) surrounding the 2010 shift in rodent community composition. As documented in [8], the 2010 transition followed a period of low abundance community-wide (A) and low plant productivity (B). Since 2010, the site has experienced two periods of drought (C) interspersed with an unusually wet period. Total rodent energy use (A) is calculated as the total energy use of all granivores on control plots (E_{totC}) in each census period. The anomaly (shown) is calculated as the difference between the total energy use in each census period and the long-term mean of total energy use. Vertical dashed lines mark the dates of major transitions in the rodent community. NDVI anomaly (B) is calculated as the difference between monthly NDVI and the long-term mean for that month. NDVI data were obtained from Landsat 5, 7, and 8 using the *ndvi* function in the R package *portralr* [? ? 9]. Drought (C) was calculated using a 12-month Standardized Precipitation Evapotranspiration index (SPEI) for all months from 1989-2020, using the Thornthwaite method to estimate potential evapotranspiration (using the R package *SPEI*; [1, 60, 6]). Values greater than 0 (blue) indicate wetter than average conditions, and values less than 0 (red) indicate drier conditions. Values between -1 and 1 (horizontal lines) are considered within normal variability for a system, while values ± 1 constitute drought [60].

APPENDIX B SECONDARY APPENDIX CONTENT

Table B-1. A sample Table using tabularx

First	Second	Third
12	45	26
17	32	93
text	51	can be there too.



Figure B-1. This is a long caption to make sure that the caption in the list-of section is correctly single space with the blank white line between captions.

Test for second appendix file.

Test for third appendix file.

REFERENCES

- [1] Santiago Beguería and Sergio M. Vicente-Serrano, *SPEI: Calculation of the Standardised Precipitation-Evapotranspiration Index*, 2017.
- [2] Ellen K. Bledsoe and S. K. Morgan Ernest, *Temporal changes in species composition affect a ubiquitous species' use of habitat patches*, *Ecology* **100** (2019), no. 11, e02869.
- [3] J. H. Brown, T. J. Valone, and C. G. Curtin, *Reorganization of an arid ecosystem in response to recent climate change*, *Proceedings of the National Academy of Sciences* **94** (1997), no. 18, 9729–9733.
- [4] James H. Brown, *Organisms and Species as Complex Adaptive Systems: Linking the Biology of Populations with the Physics of Ecosystems*, *Linking Species & Ecosystems* (Clive G. Jones and John H. Lawton, eds.), Springer US, Boston, MA, 1995, pp. 16–24.
- [5] James H. Brown and Brian A. Maurer, *Macroecology: The Division of Food and Space Among Species on Continents*, *Science* **243** (1989), no. 4895, 1145–1150.
- [6] Pablo A. Cárdenas, Erica Christensen, S. K. Morgan Ernest, David C. Lightfoot, Robert L. Schooley, Paul Stapp, and Jennifer A. Rudgers, *Declines in rodent abundance and diversity track regional climate variability in North American drylands*, *Global Change Biology* **27** (2021), no. 17, 4005–4023.
- [7] Peter Chesson, *Mechanisms of Maintenance of Species Diversity*, *Annual Review of Ecology and Systematics* **31** (2000), no. 1, 343–366.
- [8] Erica M. Christensen, David J. Harris, and S. K. Morgan Ernest, *Long-term community change through multiple rapid transitions in a desert rodent community*, *Ecology* **99** (2018), no. 7, 1523–1529.
- [9] Erica M. Christensen, Glenda M. Yenni, Hao Ye, Juniper L. Simonis, Ellen K. Bledsoe, Renata M. Diaz, Shawn D. Taylor, Ethan P. White, and S. K. Morgan Ernest, *Portalr: An R package for summarizing and using the Portal Project Data*, *Journal of Open Source Software* **4** (2019), no. 33, 1098.
- [10] Sean R. Connolly, Terry P. Hughes, David R. Bellwood, and Ronald H. Karlson, *Community Structure of Corals and Reef Fishes at Multiple Scales*, *Science* **309** (2005), no. 5739, 1363–1365.
- [11] Sarah Cusser, Christie Bahlai, Scott M. Swinton, G. Philip Robertson, and Nick M. Haddad, *Long-term research avoids spurious and misleading trends in sustainability attributes of no-till*, *Global Change Biology* **26** (2020), no. 6, 3715–3725.
- [12] Renata M. Diaz and S. K. Morgan Ernest, *Maintenance of community function through compensation breaks down over time in a desert rodent community*, Preprint, bioRxiv, October 2021.
- [13] Renata M. Diaz, Hao Ye, and S. K. Morgan Ernest, *Empirical abundance distributions are more uneven than expected given their statistical baseline*, *Ecology Letters* **24** (2021), no. 9, 2025–2039.

- [14] Rodolfo Dirzo, Hillary S. Young, Mauro Galetti, Gerardo Ceballos, Nick J. B. Isaac, and Ben Collen, *Defaunation in the Anthropocene*, *Science* **345** (2014), no. 6195, 401–406.
- [15] M. Dornelas, N. J. Gotelli, B. McGill, H. Shimadzu, F. Moyes, C. Sievers, and A. E. Magurran, *Assemblage Time Series Reveal Biodiversity Change but Not Systematic Loss*, *Science* **344** (2014), no. 6181, 296–299.
- [16] Maria Dornelas, Dawn A. T. Phillip, and Anne E. Magurran, *Abundance and dominance become less predictable as species richness decreases*, *Global Ecology and Biogeography* **20** (2011), no. 6, 832–841.
- [17] John B. Dunning, *CRC handbook of avian body masses*, 2nd ed. ed., CRC Press, Boca Raton, 2008.
- [18] S. K. Morgan Ernest, *Body size, energy use, and community structure of small mammals*, *Ecology* **86** (2005), no. 6, 1407–1413.
- [19] S. K. Morgan Ernest and James H. Brown, *Delayed Compensation for Missing Keystone Species by Colonization*, *Science* **292** (2001), no. 5514, 101–104.
- [20] S. K. Morgan Ernest, James H. Brown, Katherine M. Thibault, Ethan P. White, and Jacob R. Goheen, *Zero Sum, the Niche, and Metacommunities: Long-Term Dynamics of Community Assembly*, *The American Naturalist* **172** (2008), no. 6, E257–E269.
- [21] S. K. Morgan Ernest, Ethan P. White, and James H. Brown, *Changes in a tropical forest support metabolic zero-sum dynamics*, *Ecology Letters* **12** (2009), no. 6, 507–515.
- [22] S. K. Morgan Ernest, Glenda M. Yenni, Ginger Allington, Ellen K. Bledsoe, Erica M. Christensen, Renata M. Diaz, Keith Geluso, Jacob R. Goheen, Qinfeng Guo, Edward Heske, Douglas Kelt, Joan M. Meiners, Jim Munger, Carla Restrepo, Douglas A. Samson, Michele R. Schutzenhofer, Marian Skupski, Sarah R. Supp, Kate Thibault, Shawn Taylor, Ethan White, Hao Ye, Diane W. Davidson, James H. Brown, and Thomas J. Valone, *The Portal Project: A long-term study of a Chihuahuan desert ecosystem*, *bioRxiv* (2020), 332783.
- [23] Ingo Fetzer, Karin Johst, Robert Schäwe, Thomas Banitz, Hauke Harms, and Antonis Chatzinotas, *The extent of functional redundancy changes as species' roles shift in different environments*, *Proceedings of the National Academy of Sciences* **112** (2015), no. 48, 14888–14893.
- [24] Jonathan A. D. Fisher, Kenneth T. Frank, and William C. Leggett, *Dynamic macroecology on ecological time-scales*, *Global Ecology and Biogeography* **19** (2010), no. 1, 1–15.
- [25] Trevor S. Fristoe, *Energy use by migrants and residents in North American breeding bird communities*, *Global Ecology and Biogeography* **24** (2015), no. 4, 406–415.
- [26] Janet L. Gardner, Anne Peters, Michael R. Kearney, Leo Joseph, and Robert Heinsohn, *Declining body size: A third universal response to warming?*, *Trends in Ecology & Evolution* **26** (2011), no. 6, 285–291.

- [27] Andrew Gonzalez and Michel Loreau, *The Causes and Consequences of Compensatory Dynamics in Ecological Communities*, Annual Review of Ecology, Evolution, and Systematics **40** (2009), no. 1, 393–414.
- [28] David J. Harris, Shawn D. Taylor, and Ethan P. White, *Forecasting biodiversity in breeding birds using best practices*, PeerJ **6** (2018), e4278.
- [29] John Harte and Erica A. Newman, *Maximum information entropy: A foundation for ecological theory*, Trends in Ecology & Evolution **29** (2014), no. 7, 384–389.
- [30] Peter A. Henderson and Anne E. Magurran, *Linking species abundance distributions in numerical abundance and biomass through simple assumptions about community structure*, Proceedings of the Royal Society B: Biological Sciences **277** (2010), no. 1687, 1561–1570.
- [31] Lucina Hernández, John W. Laundré, Alberto González-Romero, Jorge López-Portillo, and Karina M. Grajales, *Tale of two metrics: Density and biomass in a desert rodent community*, Journal of Mammalogy **92** (2011), no. 4, 840–851.
- [32] C. S. Holling, *Cross-Scale Morphology, Geometry, and Dynamics of Ecosystems*, Ecological Monographs **62** (1992), no. 4, 447–502.
- [33] J. E. Houlahan, D. J. Currie, K. Cottenie, G. S. Cumming, S. K. M. Ernest, C. S. Findlay, S. D. Fuhlendorf, R. D. Stevens, T. J. Willis, I. P. Woiwod, and S. M. Wondzell, *Compensatory dynamics are rare in natural ecological communities.*, Proceedings of the National Academy of Sciences. 104(9): 3273-3277 (2007).
- [34] Stephen P. Hubbell, *The Unified Neutral Theory of Biodiversity and Biogeography (MPB-32)*, Princeton University Press, 2001.
- [35] Brent B. Hughes, Rodrigo Beas-Luna, Allison K. Barner, Kimberly Brewitt, Daniel R. Brumbaugh, Elizabeth B. Cerny-Chipman, Sarah L. Close, Kyle E. Coblenz, Kristin L. de Nesnera, Sarah T. Drobnič, Jared D. Figurski, Becky Focht, Maya Friedman, Jan Freiwald, Kristen K. Heady, Walter N. Heady, Annaliese Hettinger, Angela Johnson, Kendra A. Karr, Brenna Mahoney, Monica M. Moritsch, Ann-Marie K. Osterback, Jessica Reimer, Jonathan Robinson, Tully Rohrer, Jeremy M. Rose, Megan Sabal, Leah M. Segui, Chenchen Shen, Jenna Sullivan, Rachel Zuercher, Peter T. Raimondi, Bruce A. Menge, Kirsten Grorud-Colvert, Mark Novak, and Mark H. Carr, *Long-Term Studies Contribute Disproportionately to Ecology and Policy*, BioScience **67** (2017), no. 3, 271–281.
- [36] Forest Isbell, Vincent Calcagno, Andy Hector, John Connolly, W. Stanley Harpole, Peter B. Reich, Michael Scherer-Lorenzen, Bernhard Schmid, David Tilman, Jasper van Ruijven, Alexandra Weigelt, Brian J. Wilsey, Erika S. Zavaleta, and Michel Loreau, *High plant diversity is needed to maintain ecosystem services*, Nature **477** (2011), no. 7363, 199–202.
- [37] Douglas A. Kelt, *Comparative ecology of desert small mammals: A selective review of the past 30 years*, Journal of Mammalogy **92** (2011), no. 6, 1158–1178.

- [38] Douglas A. Kelt, Jaclyn R. Aliperti, Peter L. Meserve, W. Bryan Milstead, M. Andrea Previtali, and Julio R. Gutierrez, *Energetic compensation is historically contingent and not supported for small mammals in South American or Asian deserts*, Ecology **96** (2015), no. 6, 1702–1712.
- [39] S. R. Kerr and L. M. Dickie, *The Biomass Spectrum: A Predator-Prey Theory of Aquatic Production*, Columbia University Press, November 2001.
- [40] John H. Lawton, *What Do Species Do in Ecosystems?*, Oikos **71** (1994), no. 3, 367–374.
- [41] ———, *Are There General Laws in Ecology?*, Oikos **84** (1999), no. 2, 177.
- [42] Mathew A. Leibold, Jonathan M. Chase, and S. K. Morgan Ernest, *Community assembly and the functioning of ecosystems: How metacommunity processes alter ecosystems attributes*, Ecology **98** (2017), no. 4, 909–919.
- [43] Russell V. Lenth, *Emmeans: Estimated Marginal Means, aka Least-Squares Means*, 2021.
- [44] Kenneth J. Locey and Ethan P. White, *How species richness and total abundance constrain the distribution of abundance*, Ecology Letters **16** (2013), no. 9, 1177–1185.
- [45] Michel Loreau, *Does functional redundancy exist?*, Oikos **104** (2004), no. 3, 606–611.
- [46] Brian J. McGill, *The what, how and why of doing macroecology*, Global Ecology and Biogeography **28** (2019), no. 1, 6–17.
- [47] Brian J. McGill, Maria Dornelas, Nicholas J. Gotelli, and Anne E. Magurran, *Fifteen forms of biodiversity trend in the Anthropocene*, Trends in Ecology & Evolution **30** (2015), no. 2, 104–113.
- [48] Brian Keith McNab, *Ecological factors affect the level and scaling of avian BMR*, Comparative Biochemistry and Physiology Part A: Molecular & Integrative Physiology **152** (2009), no. 1, 22–45.
- [49] Hélène Morlon, Ethan P. White, Rampal S. Etienne, Jessica L. Green, Annette Ostling, David Alonso, Brian J. Enquist, Fangliang He, Allen Hurlbert, Anne E. Magurran, Brian A. Maurer, Brian J. McGill, Han Olff, David Storch, and Tommaso Zillio, *Taking species abundance distributions beyond individuals*, Ecology Letters **12** (2009), no. 6, 488–501.
- [50] Kenneth A. Nagy, *Field metabolic rate and body size*, Journal of Experimental Biology **208** (2005), no. 9, 1621–1625.
- [51] Jeffrey C. Nekola and James H. Brown, *The wealth of species: Ecological communities, complex systems and the legacy of Frank Preston*, Ecology Letters **10** (2007), no. 3, 188–196.
- [52] Keith L. Pardieck, David J. Ziolkowski, Michael Lutmerding, Veronica Aponte, and Marie-Anne Hudson, *North American Breeding Bird Survey Dataset 1966 - 2018, version 2018.0*, 2019.

- [53] Owen L. Petchey and Andrea Belgrano, *Body-size distributions and size-spectra: Universal indicators of ecological status?*, *Biology Letters* **6** (2010), no. 4, 434–437.
- [54] Jose Pinheiro, Douglas Bates, Saikat DebRoy, Deepayan Sarkar, and R Core Team, *Nlme: Linear and Nonlinear Mixed Effects Models*, 2020.
- [55] R Core Team, *R: A Language and Environment for Statistical Computing*, R Foundation for Statistical Computing, 2020.
- [56] Quentin D. Read, John M. Grady, Phoebe L. Zarnetske, Sydne Record, Benjamin Baiser, Jonathan Belmaker, Mao-Ning Tuanmu, Angela Strecker, Lydia Beaudrot, and Katherine M. Thibault, *Among-species overlap in rodent body size distributions predicts species richness along a temperature gradient*, *Ecography* **41** (2018), no. 10, 1718–1727.
- [57] Jordan S. Rosenfeld, *Functional redundancy in ecology and conservation*, *Oikos* **98** (2002), no. 1, 156–162.
- [58] Aafke M. Schipper, Jonathan Belmaker, Murilo Dantas de Miranda, Laetitia M. Navarro, Katrin Böhning-Gaese, Mark J. Costello, Maria Dornelas, Ruud Foppen, Joaquín Hortal, Mark A. J. Huijbregts, Berta Martín-López, Nathalie Pettorelli, Cibele Queiroz, Axel G. Rossberg, Luca Santini, Katja Schifflers, Zoran J. N. Steinmann, Piero Visconti, Carlo Rondinini, and Henrique M. Pereira, *Contrasting changes in the abundance and diversity of North American bird assemblages from 1971 to 2010*, *Global Change Biology* **22** (2016), no. 12, 3948–3959.
- [59] Oswald J. Schmitz, Christopher C. Wilmers, Shawn J. Leroux, Christopher E. Doughty, Trisha B. Atwood, Mauro Galetti, Andrew B. Davies, and Scott J. Goetz, *Animals and the zoogeochimistry of the carbon cycle*, *Science* (2018).
- [60] Ingrid J. Slette, Alison K. Post, Mai Awad, Trevor Even, Arianna Punzalan, Sere Williams, Melinda D. Smith, and Alan K. Knapp, *How ecologists define drought, and why we should do better*, *Global Change Biology* **25** (2019), no. 10, 3193–3200.
- [61] Felisa A. Smith, Rosemary E. Elliott Smith, S. Kathleen Lyons, and Jonathan L. Payne, *Body size downgrading of mammals over the late Quaternary*, *Science* **360** (2018), no. 6386, 310–313.
- [62] Sarah Supp, *Manipulated Animal Community Database*, March 2014.
- [63] Rebecca C. Terry and Rebecca J. Rowe, *Energy flow and functional compensation in Great Basin small mammals under natural and anthropogenic environmental change*, *Proceedings of the National Academy of Sciences* **112** (2015), no. 31, 9656–9661.
- [64] Katherine M. Thibault and James H. Brown, *Impact of an extreme climatic event on community assembly*, *Proceedings of the National Academy of Sciences of the United States of America* **105** (2008), no. 9, 3410–3415.

- [65] Katherine M. Thibault, S. K. Morgan Ernest, and James H. Brown, *Redundant or complementary? Impact of a colonizing species on community structure and function*, *Oikos* **119** (2010), no. 11, 1719–1726.
- [66] Katherine M. Thibault, Ethan P. White, Allen H. Hurlbert, and S. K. Morgan Ernest, *Multimodality in the individual size distributions of bird communities*, *Global Ecology and Biogeography* **20** (2011), no. 1, 145–153.
- [67] Leigh Van Valen, *A new evolutionary law*, *Evolutionary Theory* **1** (1973), no. 1, 1–30.
- [68] Brian Walker, *Conserving Biological Diversity through Ecosystem Resilience*, *Conservation Biology* **9** (1995), no. 4, 747–752.
- [69] Brian H. Walker, *Biodiversity and Ecological Redundancy*, *Conservation Biology* **6** (1992), no. 1, 18–23.
- [70] R. M. Warwick and K. R. Clarke, *Relearning the ABC: Taxonomic changes and abundance/biomass relationships in disturbed benthic communities*, *Marine Biology* **118** (1994), no. 4, 739–744.
- [71] Ethan P. White, *Two-phase species-time relationships in North American land birds*, *Ecology Letters* **7** (2004), no. 4, 329–336.
- [72] Ethan P. White, S. K. Morgan Ernest, and Katherine M. Thibault, *Trade-offs in Community Properties through Time in a Desert Rodent Community.*, *The American Naturalist* **164** (2004), no. 5, 670–676.
- [73] Ethan P. White, S.K. Morgan Ernest, Andrew J. Kerkhoff, and Brian J. Enquist, *Relationships between body size and abundance in ecology*, *Trends in Ecology & Evolution* **22** (2007), no. 6, 323–330.
- [74] John W. Williams and Stephen T. Jackson, *Novel climates, no-analog communities, and ecological surprises*, *Frontiers in Ecology and the Environment* **5** (2007), no. 9, 475–482.
- [75] Hao Ye, Ellen K. Bledsoe, Renata Diaz, S. K. Morgan Ernest, Juniper L. Simonis, Ethan P. White, and Glenda M. Yenni, *Macroecological Analyses of Time Series Structure*, Zenodo, May 2020.
- [76] Jian D. L. Yen, James R. Thomson, Jonathan M. Keith, David M. Paganin, Erica Fleishman, David S. Dobkin, Joanne M. Bennett, and Ralph Mac Nally, *Balancing generality and specificity in ecological gradient analysis with species abundance distributions and individual size distributions: Community distributions along environmental gradients*, *Global Ecology and Biogeography* **26** (2017), no. 3, 318–332.
- [77] Hillary S. Young, Douglas J. McCauley, Mauro Galetti, and Rodolfo Dirzo, *Patterns, Causes, and Consequences of Anthropocene Defaunation*, *Annual Review of Ecology, Evolution, and Systematics* **47** (2016), no. 1, 333–358.

BIOGRAPHICAL SKETCH

Renata Diaz grew up surrounded by the fields of eastern Colorado and the forests of New England, in a family of enthusiastic puzzle solvers and natural historians. During her undergraduate work in Ecology and Evolutionary Biology at Princeton University, she developed a keen interest in the interplay between theoretical, computational, and empirical modalities in ecology. For her senior thesis, she combined field experiments with a mathematical model to predict how the joint effects of large mammalian herbivores, small mammalian seed predators, and historical legacies of human-wildlife interactions modulate the spatial distribution of trees in East African savannas. From 2015 to 2017, she continued to explore dimensions of ecology as a research assistant in the Staver Lab at Yale University (2015-2016), a field intern with the Ecology of Bird Loss Project (2016), and a spatial data analysis intern in the Global Change Ecology lab at the Missouri Botanic Garden (2017). In 2017, she joined the Ernest and weecology labs at the University of Florida to pursue a PhD in macroecology, combining field work associated with The Portal Project with data- and computationally- intensive synthesis, software development projects, and intellectually adventurous theoretical pursuits.